

# 1 Conceptualising surface water-groundwater exchange in braided 2 river systems

3 Scott R. Wilson<sup>1</sup>, Jo Hoyle<sup>2</sup>, Richard Measures<sup>2</sup>, Antoine Di Ciacca<sup>1</sup>, Leanne K. Morgan<sup>3</sup>, Eddie  
4 W. Banks<sup>4</sup>, Linda Robb<sup>1</sup>, and Thomas Wöhling<sup>1,5</sup>

5 <sup>1</sup>Environmental Research, Lincoln Agritech, Lincoln University, New Zealand

6 <sup>2</sup>National Institute of Water & Atmospheric Research, Christchurch, New Zealand

7 <sup>3</sup>Waterways Centre for Freshwater Management, University of Canterbury, Christchurch, New Zealand

8 <sup>4</sup>National Centre for Groundwater Research & Training & College of Science & Engineering, Flinders University,  
9 Australia

10 <sup>5</sup>Chair of Hydrology, Technische Universität Dresden, Dresden, Germany

11 *Correspondence to:* Scott R. Wilson (scott.wilson@lincolnagritech.co.nz)

## 12 13 **Abstract**

14 Braided rivers can provide substantial recharge to regional aquifers, with flow exchange  
15 between surface water and groundwater occurring at a range of spatial and temporal scales.

16 However, the difficulty of measuring and modelling these complex and dynamic river  
17 systems has hampered process understanding and the upscaling necessary to quantify these  
18 fluxes. This is due to an incomplete understanding of the hydrogeological structures which  
19 control river-groundwater exchange. In this paper we present a new conceptualisation of  
20 subsurface processes in braided rivers based on observations of the main losing reaches of  
21 three braided rivers in New Zealand.

22 The conceptual model is based on a range of data including lidar, bathymetry, coring,  
23 particle size distribution, groundwater, and temperature monitoring, radon-222, electrical  
24 resistivity tomography, and fibre optic cables. The combined results indicate that sediments  
25 within the recently active river braidplain are distinctive, with sediments that are poorly  
26 consolidated and better sorted compared to adjacent deposits from the historical braidplain  
27 which become successively consolidated and intermixed with flood silt deposits due to  
28 overbank flow.

29 A distinct sedimentary unconformity, combined with the presence of geomorphologically  
30 distinct lateral boundaries, suggests that a “braided plain aquifer” forms within the active river  
31 braided plain through the process of sediment mobilisation during flood events.

32 This braided plain aquifer concept introduces a shallow storage reservoir to the river system,  
33 which is distinct from the regional aquifer system, and mediates the exchange of flow  
34 between individual river channels and the regional aquifer. The implication of the new  
35 concept is that surface water-groundwater exchange occurs at two spatial scales. The first is  
36 hyporheic and parafluvial exchange between the river and braided plain aquifer. The second is  
37 exchange between the braided plain aquifer and regional aquifer system. Exchange at both  
38 scales is influenced by the state of hydraulic connection between the respective water  
39 bodies. This conceptualisation acknowledges braided rivers as whole “river systems”,  
40 consisting of channels, and gravel aquifer reservoir.

41 This work has important implications for understanding how changes in river management  
42 (e.g., surface water extraction, bank training and gravel extraction) and morphology may  
43 impact groundwater recharge, and potentially on flow, temperature attenuation, and  
44 ecological resilience during dry conditions.

45

## 46 **1.0 Introduction**

47 This study is motivated by the need to understand processes and quantify losses from  
48 braided river systems to alluvial aquifers. In New Zealand more than 150 river systems are  
49 thought to have braided reaches (Brower et al., 2024), which provide a substantial  
50 component of recharge to alluvial aquifers. For example, in the case of the Wairau Aquifer,  
51 it has been estimated recharge is sourced almost exclusively from the Wairau River  
52 (Wöhling et al. 2018).

53 Braided rivers are spatially complex, dynamic hydrologic environments which are not easily  
54 measured using field techniques or represented by numerical models. The determination of  
55 flow exchanges between the river and groundwater in such a hydrologically complex and  
56 morphologically dynamic environment is difficult because of their spatial and temporal flow  
57 complexity, numerous and changing number of channels, dynamic bathymetry, coarse  
58 substrate, and tendency for loss of field installations during high flow events. The  
59 complexity of this challenge demands a collaborative effort that leverages the strengths of a  
60 diverse range of disciplines to develop a comprehensive and holistic understanding of the  
61 problem.

62 Many authors have studied surface-aquifer exchanges, and several reviews have been  
63 conducted on available techniques for measuring exchanges for alluvial rivers in general  
64 (Kalbus et al. 2006, González-Pinzón et al. 2015, Brunner et al. 2017), ephemeral rivers at  
65 different spatial scales (Banks et al., 2011, Shanafield and Cook 2014), and braided rivers  
66 (Coluccio and Morgan, 2019). Based on these reviews, there is a tendency for previous  
67 studies to focus on quantifying exchange fluxes prior to understanding the hydrological  
68 processes that influence the exchange. Ward and Packman (2019) suggest that despite the  
69 large amount of research on river-groundwater exchanges, an accurate predictive,  
70 transferable understanding of the river corridor is lacking. Indeed, a conceptualisation of  
71 how braided rivers relate to their underlying groundwater systems is lacking (Coluccio and  
72 Morgan, 2019). This has led to ambiguity in what measured exchanges represent, and  
73 difficulty in trying to represent braided rivers within aquifer scale models.

74 The aim of this paper is to formulate a conceptualisation of braided river exchange  
75 processes at both the local (reach) and sub-catchment (aquifer) scale. This conceptualisation  
76 provides a framework for both providing context for field measurements of flow exchange

77 to be interpreted, and the potential for representation of local scale processes in sub-  
78 catchment models. Incorporating these local scale processes is vital to predict how changes  
79 in the river system can impact groundwater recharge.

80 The conceptualisation presented here was developed based on field observations but, for  
81 clarity of explanation, we introduce the conceptual framework first and then present the  
82 supporting evidence. Our working definition for hyporheic exchange is local bed-scale  
83 interaction that occurs within a single channel (e.g., a single riffle), whereas parafluvial  
84 exchange occurs between individual channels at larger scales (across a bar or further). We  
85 also distinguish between a river as a series of wetted channels, and a “river system”, which  
86 consists of wetted channels plus subsurface flow through the associated braidplain gravels.  
87 “Braidplain” refers to the lateral extent occupied by the river braids, old bar surfaces and  
88 abandoned channels (Warburton, 1996; Gray et al., 2016; Brower et al., 2023). The extent of  
89 wetted channels and recently reworked bed material (bare gravel) at a given point in time  
90 defines the “active braidplain”, which also has potential to shift laterally. Lateral adjustment  
91 of the active braidplain may be limited by hillslope margins, terraces or, in managed rivers,  
92 by rock revetments or artificial stop banks (levees) which are typically protected with  
93 vegetative buffers. We refer to the extent within which our study rivers can currently adjust  
94 as the “contemporary braidplain”, acknowledging that in two of our study rivers (Wairau  
95 and Ngaruroro) the contemporary braidplain margins are controlled by engineered flood  
96 defences which have narrowed the natural braidplain such that almost the entire  
97 contemporary braidplain is active.

98

## 99 **2.0 Review of existing concepts**

100 The prevailing conceptualisation for gravel bed rivers in general consists of a surface  
101 channel with an associated bed with some hydraulic resistance (Schälchli 1992, Wu and  
102 Huang 2000) which exchanges water with an associated fluvial or alluvial aquifer (Stanford  
103 and Ward 1993, Poole and Berman 2001). Within the alluvial aquifer lies a hyporheic zone  
104 which functions as an interface between groundwater and surface waters (Stanford and  
105 Ward 1993, Poole and Berman 2001, Boano et al. 2014). The extent of the hyporheic zone is  
106 defined by its function or process of interest, which can be physical, chemical, biological, or  
107 a combination of functions (Ward 2015). Accordingly, the vertical or lateral boundaries of  
108 the hyporheic zone are transient and flexible, and not easily defined spatially (White 1993,  
109 Boulton et al. 1998, Ward 2015). From a hydrological perspective, the hyporheic zone has  
110 been defined as the extent to which surface water enters the high porosity subsurface  
111 beneath and lateral to a stream and returns to the stream surface farther downstream  
112 (Harvey and Wagner, 2000). Authors have suggested the hyporheic zone as extending from  
113 the upper few centimetres of sediment (Boulton et al. 1998, Sophocleous 2002) to larger  
114 scales (km<sup>3</sup>) constituting a hyporheic corridor (Stanford and Ward 1993). Valett et al. (1996)  
115 predict the extent of the hyporheic zone to be related to catchment lithology, with  
116 interaction being more extensive in sites with higher alluvial hydraulic conductivity, whereas  
117 Boano et al. (2008) predict the infiltration depth to be related to bedform for any given  
118 hydraulic conductivity.

119 An additional, ecological, concept is that of a riparian zone (Steiger et al. 2005). This extends  
120 river margins beyond the active channel to include the biosphere supported by and  
121 including recent fluvial landforms and inundated or saturated by bank discharge (Hupp and  
122 Osterkamp 1996). Other authors have considered the presence of a parafluvial zone  
123 situated between the hyporheic zone (beneath the river channel) and riparian zone (Holmes

124 et al. 1994) which accommodates longer flow paths within the alluvium adjacent to the  
125 stream (Bourke et al. 2014, Cartwright and Hoffmann 2016). Our interpretation of the  
126 parafluvial zone is that it constitutes exchange flow within the alluvial aquifer at spatial and  
127 temporal scales beyond what is considered hyporheic.

128 From a hydrological perspective of braided rivers, the framework that emerges from the  
129 prevailing concepts is one where river-groundwater exchange occurs within an alluvial  
130 aquifer which conveys both hyporheic and parafluvial flowpaths. The proportion of these  
131 flowpath components theoretically depends on the degree to which there is a net loss or  
132 gain in river channel flow. However, the interpretation of river-groundwater exchanges  
133 becomes challenging in a braided river which comprises multiple channels within an alluvial  
134 aquifer. Harvey and Gooseff (2015), Barthel and Banzhaf (2016) and Ward and Packman  
135 (2019) propose that exchange fluxes be considered at different spatial scales: point, local,  
136 sub-catchment, and regional. Following this approach, exchange within individual river  
137 braids or channels can be considered to occur at the point-scale, and the sum of all braids  
138 within a river reach as a local-scale interaction. While process understanding can be  
139 observed and fluxes quantified at the point and local scale, it is imperative to enable an  
140 upscaling of observed processes so that fluxes can be estimated for at least the sub-  
141 catchment (aquifer) scale.

142 Previous work on subsurface structure in braided rivers has tended to focus on the role of  
143 bed material heterogeneity. A significant body of literature exists to describe braided river  
144 deposits via morphology (Huber and Huggenberger 2016), sedimentology (Huggenberger  
145 and Regli 2006, Theel et al. 2020), geophysics (Pirrot et al. 2019), and modelling approaches  
146 (Pirrot et al. 2014; 2015, Brunner et al. 2017, Schilling et al. 2022). To date, no conceptual  
147 model has been posed for how a braided river and its associated braidplain gravels (alluvial

148 aquifer) relate to those of the underlying regional aquifer. While the structural components  
149 of river-groundwater interaction have been identified by previous authors (e.g. Poole and  
150 Berman 2001, Steiger et al. 2005), the identification of clear spatial boundaries between  
151 structural elements has been missing. From a hydrological perspective of understanding  
152 surface water-groundwater interaction, this creates a problem of where the river system  
153 ends, and where the regional groundwater system begins. The uncertainty related to this  
154 lack of spatial definition transfers to the interpretation of field data, whether a sample is  
155 representative of river channel flow, alluvial aquifer (hyporheic or parafluvial zones), or  
156 regional groundwater.

157 Consequently, representation of braided rivers in numerical models is problematic since  
158 their complexity is not readily captured by a simple conceptualisation. Water exchanges can  
159 potentially be simulated realistically using a fully coupled hydrological model such as  
160 HydroGeoSphere (Therrien et al. 2010, Brunner and Simmons 2012). However, the data  
161 required to parametrise such a model, and the computational demands of the detailed  
162 mesh required to simulate exchanges in braided rivers make this approach only suitable for  
163 point and local scale studies. Furthermore, braided river morphology is so dynamic that a  
164 new bed morphology would be required following each significant flood event. In recent  
165 years, two approaches to simulate the transitions of dynamic bed morphology and  
166 sediments on river-groundwater exchanges have been tested. The first approach applied  
167 the ensemble Kalman filter and areal imagery to assimilate river bed topography and to  
168 update aquifer hydraulic conductivities in a HydroGeoSphere model for a 2-km section of  
169 the Emme River in Switzerland (Tang et al. 2018). The data assimilation scheme strongly  
170 improved predictions of post-flood hydraulic states of the system. The second approach  
171 proposed a pilot point parametrization scheme where both the aquifer properties (hydraulic

172 conductivity) and the location of the pilot points are inferred, e.g. from river-bed training  
173 images (Khambhammettu et al. 2020). The corresponding Traveling Pilot points (TRIPS)  
174 scheme could potentially be used to describe the transition between discrete states of river  
175 morphology. To some extent these approaches enable the application of fully integrated 3D  
176 models in dynamic river environments of appropriate scale, although their application in a  
177 larger river system or at a larger scale is untested.

178 The simple river structure offered by the Streamflow-Routing (SFR, Niswonger and Prudic,  
179 2005) and River (Harbaugh, 2005) packages in MODFLOW represent the river as a flux  
180 boundary condition with vertical flow impedance in the bed expressed by a lumped  
181 parameter termed 'streambed conductance'. Previous authors have shown that the concept  
182 of a streambed resistance concentrating all pressure losses, as implemented in MODFLOW,  
183 is questionable in many cases (Anderson 2005, Rushton 2007, Morel-Seytoux et al. 2018, Di  
184 Ciacca et al. 2019). Moreover, even if such a streambed exists, a major physical issue with a  
185 lumped parameter approach is that streambed conductance values in the field are not  
186 homogenous, but vary spatially (Cardenas and Zlotnik 2003, Zhou et al. 2014, Pryshlak et al.  
187 2015, Laube et al. 2018) and temporally (Levy et al., 2011, Wu et al. 2015). In a braided  
188 river, bed material typically consists of a heterogeneous mixture of cobbles, gravels, and  
189 sands, which can have similar characteristics to alluvial sediments located several metres  
190 beneath the bed. Therefore, the streambed conductance concept seems inappropriate to  
191 represent surface water-groundwater exchange in braided river systems.

192 Different modelling approaches have been trialled to represent braided rivers in New  
193 Zealand. White et al. (2012) conducted a steady state water balance approach to determine  
194 flow losses for a reach of the Waimakariri River. Exchanges between individual channels and  
195 the adjacent alluvial aquifer were determined via mass balance, although the subsurface



196 components of the exchange were not explicitly described. An alternative approach by  
197 Wöhling et al. (2018, 2020) simulated dynamic Wairau River exchanges at the sub-  
198 catchment scale using MODFLOW. In this case, the braided nature of the river was not  
199 considered, and the river was represented by the SFR package using a stage-width-flow  
200 relationship derived from a representative channel morphology. While this model fitted  
201 river flux and groundwater level data well, the approach employed a streambed  
202 conductance model, which is difficult to reconcile with the river morphology and bed  
203 sediment seen in the field. A particular drawback of the SFR package is its inability to  
204 represent the hyporheic or parafluvial exchange fluxes observed at the point or local scale.  
205 While the Waimakariri and Wairau modelling studies are relatively comprehensive, in both  
206 cases, an understanding of subsurface structure is missing from the river representation.  
207 This lack of knowledge about the structural controls on subsurface flow in the braided river  
208 environment needs clarification to understand what measured and modelled river-  
209 groundwater exchanges represent. In doing this, a more physically realistic method for  
210 representing braided rivers in numerical surface water-groundwater flow models may be  
211 achieved.

212

### 213 **3.0 Proposed conceptualisation**

214 A conceptual framework is proposed which captures the key elements of water exchanges  
215 in a braided river system. This conceptualisation builds on the previous work of Fox and  
216 Durnford (2003) and Brunner et al. (2009a and b) and recognises that the hydrological  
217 controls on river-groundwater exchange occur at two distinct interfaces within a braidplain  
218 system. Specifically, these two exchange processes can be summarised as:

- 219 1. River channel ↔ braidplain aquifer (hyporheic and/or parafluvial exchange)

220 2. Braidplain aquifer ↔ regional aquifer (“river system” - groundwater exchange)

221 The first exchange interface is within the active braidplain, and occurs between individual

222 river channels (braids) and the local shallow water-table in the river bed sediments, and

223 occurs at the point or local scale. We term the water stored within these river bed

224 sediments the “braidplain aquifer” (BPA), which facilitates hyporheic and parafluvial flow.

225 For a perennially flowing river, the BPA will retain some degree of saturation throughout the

226 year, although unsaturated conditions may occur in the case of intermittent or ephemeral

227 rivers if there are prolonged periods with no river flow. Individual river braids can be in

228 hydraulic connection (gaining or losing), disconnection, or a transitional state relative to the

229 BPA. At the active braidplain interface, all possible river exchange processes can occur

230 regardless of the hydraulic relationship between the BPA and surrounding regional water

231 table. The second exchange interface occurs at both the local (reach) and sub-catchment

232 (aquifer) scale, between the BPA and regional water table.

233 Central to this conceptualisation is the presence of a distinct BPA immediately beneath the

234 river surface which facilitates exchange at these two interfaces. A similar term “braided-

235 river aquifer” has been used by previous authors (Pirrot et al. 2015), although we have not

236 found an associated definition. The BPA functions as a storage medium to exchange water

237 between the river and regional aquifer in braided river systems. Direct exchange of water

238 between the river and regional aquifer can only occur if the river channel is in direct contact

239 with the regional aquifer (i.e., where the surface water extends to the boundary of the BPA,

240 for example where a channel follows the lateral margin of the BPA, or there is a connection

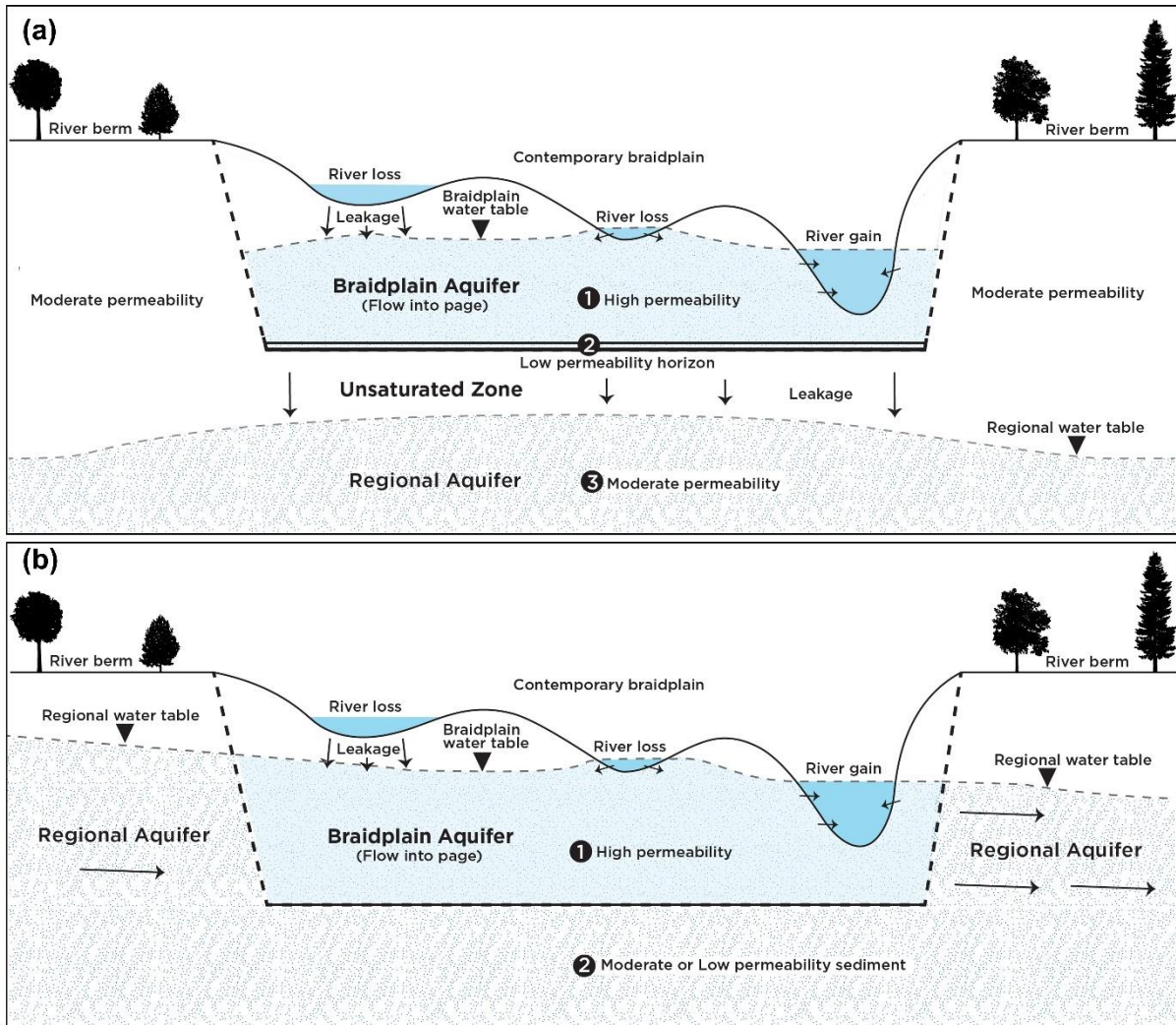
241 at the base of a deep scour pool).

242 A key feature of the BPA is its extremely high transmissivity, which is a product of the highly

243 dynamic nature of braided rivers. Bedload transport during flood events causes braids to

244 form, migrate, and be abandoned; processes that re-work the river bed sediments (Bristow  
245 and Best, 1993; Reinfelds and Nanson, 1993). This reworking process strips most fine  
246 sediment (silts and clays) from the river bed, as the shear stresses during floods are too high  
247 for these size fractions to be deposited except in vegetated areas and backwaters. The  
248 result is a braidplain deposit of high transmissivity lag gravels. High transmissivity combined  
249 with the relatively large bed slope of braided rivers and the presence of multiple braids for  
250 water exchange produces a groundwater flow path which is sub-parallel to the  
251 contemporary braidplain, regardless of the regional groundwater flow direction.

252 Conceptual diagrams have been drawn for situations where the BPA is hydraulically  
253 disconnected from (Figure 1a) and connected to (Figure 1b) the regional aquifer. The first  
254 case (Figure 1a) consists of three functional lithological layers representing a BPA which is  
255 hydraulically disconnected from an underlying regional aquifer by an unsaturated zone. In  
256 this case, water moves vertically from the BPA to the regional aquifer under a unit hydraulic  
257 gradient. A minimum of three layers is required for an unsaturated zone to develop (Fox and  
258 Durnford, 2003), and there must be a sufficient transmissivity contrast between the  
259 impeding horizon and underlying sediments (Brunner et al., 2009a and b). It should be  
260 noted that braided river deposits are lithologically variable and complex, and in most cases  
261 only two functional layers are required due to stratification in the underlying sediments.



262

263 **Figure 1.** Conceptualisation for a braidplain aquifer which is (a) hydraulically disconnected  
 264 from or transitional with the regional groundwater system, and (b) hydraulically connected  
 265 to the regional groundwater system.

266

267 A hydraulically disconnected river system setting shares features in common with  
 268 intermittent or ephemeral rivers (Shanfield et al. 2021). Infiltration to the regional  
 269 is regulated by the vertical resistance of lower permeability sediments and the hydraulic  
 270 head in the BPA. If the BPA is fully saturated across the contemporary braidplain, the rate of  
 271 infiltration to the regional aquifer will be steady because the braidplain has reached a  
 272 maximum wetted area. In this condition, some minor temporal infiltration variability will

273 occur due to changing water levels in the BPA. Under ephemeral conditions, the saturated  
274 extent of the BPA decreases longitudinally, and locally laterally, during drying phases in  
275 response to extended periods of low river flow. The combined reduction in head and  
276 saturated area of wetted braidplain result in considerably less infiltration to the regional  
277 aquifer (Di Ciacca et al. 2023).

278 The second case is a setting where the river is hydraulically connected to the regional  
279 aquifer system (Figure 1b). A minimum of two lithological units are present, a high  
280 transmissivity BPA and regional aquifer (1) overlying less permeable sediments (2) which  
281 impede vertical flow. The combination of these two factors creates an anisotropy, with  
282 preferential flow in the lateral direction. Hydraulically gaining conditions will occur in  
283 situations where regional water levels are elevated by low permeability boundaries (i.e. the  
284 presence of bedrock) on one or both sides of the river, or at middle to distal positions on  
285 alluvial fans where regional groundwater levels are closer to the land surface.

286 For a hydraulically connected river system (braids + BPA), the hydraulic gradient is no longer  
287 vertical, as it is for the hydraulically disconnected scenario, but variable, with the exchange  
288 rate governed by the relative hydraulic gradient between the braidplain and regional  
289 aquifers. Thus, groundwater inflow to the BPA or discharge to the regional aquifer can occur  
290 laterally along both margins of the braidplain, as well as vertically through BPA base. The  
291 setting can also be asymmetric, with inflow on one margin, and outflow on the other (as  
292 shown in Figure 1b), with the total river system water balance being gaining or losing, or  
293 having no flow along one margin due to the presence of bedrock.

294 While the hydraulically connected situation is simpler structurally, relative to the  
295 disconnected situation, exchange between the braidplain and regional aquifers is more  
296 complex. In this case (Figure 1b), water exchange is governed by the hydraulic gradient

297 between the two aquifers, the transmissivity of both aquifers, and the vertical hydraulic  
298 conductivity of the underlying sediments. Once water exits the BPA in a losing reach, it will  
299 not return unless it is re-routed back to the river system by a reversal of the hydraulic  
300 gradient.

301 The sedimentological features and groundwater-surface water interaction concepts  
302 associated within the contemporary braidplain have been identified and detailed by  
303 previous authors (e.g., Huggenberger et al. 1998). Regardless of the nature of the  
304 relationship between the braidplain and regional aquifers, the braidplain gravels have a  
305 higher transmissivity than both the adjacent and underlying sediments because of repeated  
306 reworking of the braidplain gravels during high flow events. Hyporheic and parafluvial flow  
307 occurs within these highly transmissive BPA sediments, subparallel to the river flow  
308 direction, with individual braids acting as recharge or discharge boundaries. As such, the  
309 local hydraulic gradient and groundwater flux are largely influenced by river bathymetry.

310

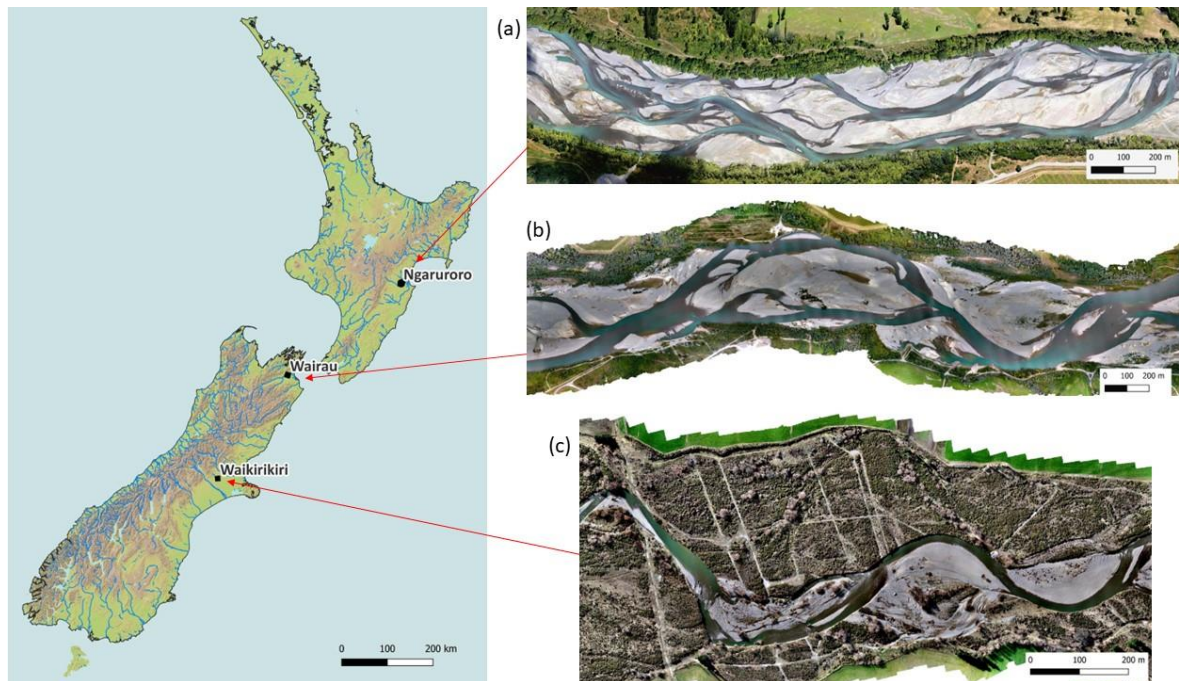
## 311 **4.0 Locations and methods for concept validation**

### 312 *4.1 Catchment descriptions*

313 The conceptualisation presented here is based on field observations of the main losing  
314 reaches of three braided rivers in the drier eastern part of New Zealand (Figure 2). These  
315 are, from north to south, the Ngaruroro (a), Wairau (b), and the Waikirikiri (c, also known as  
316 the Selwyn). These study areas were selected to take advantage of the potential for  
317 hydrological separation afforded by dominantly losing river reaches. The downward  
318 hydraulic gradient, and potential hydrological separation between channel, bed gravels and  
319 regional aquifer enable the possibility for different structural and hydrological components

320 to be identified. Summary hydrological and geomorphological statistics for the three study  
321 sites and their source catchments are shown in Table 1.

322



323

324 **Figure 2.** Location of the three study rivers and their aerial images

325

326 The Ngaruroro River is 164 km long, and has its headwaters in the Kaweka, Kaimanawa, and  
327 Ruahine ranges on the main divide of the North Island. The 3 km long study reach is located  
328 at the margin of the Heretaunga plain between Roy's Hill and Fernhill and is the main  
329 recharge source for the Heretaunga alluvial aquifer system (David and Brown, 1997). A  
330 long-term flow monitoring site at Fernhill (70 years), situated at the lower end of our study  
331 reach, has recorded a mean flow of  $40 \text{ m}^3 \cdot \text{s}^{-1}$  and mean annual peak flow of  $1546 \text{ m}^3 \cdot \text{s}^{-1}$ . The  
332 Ngaruroro study reach is in a natural depositional zone within the catchment (i.e., bedload  
333 into the reach exceeds that leaving the reach). This reach typically has 3 braids, with the  
334 active braidplain confined between willow plantings.

335

336 The Wairau River (Wöhling et al., 2018 and 2020) is 170 km long, and has its headwaters in  
337 the alpine Spencer Range on the main divide of the South Island. As such, the Wairau  
338 receives considerable source water from rain at higher elevations, producing a mean flow of  
339  $100 \text{ m}^3 \cdot \text{s}^{-1}$ , and high mean annual peak flow of  $1911 \text{ m}^3 \cdot \text{s}^{-1}$  (63 years of record at SH1). The  
340 Wairau River is also “flashy”, with over ten events exceeding three times the median flow  
341 annually (FRE3, Booker 2013). The 2.2 km long study reach is in the middle section of the  
342 Wairau Plain, between Jeffries and Giffords roads. This study reach typically has 2 braids and  
343 the active braidplain is confined between engineered rock revetments and groynes. Bedload  
344 flux into and out of this reach is approximately equal (bedload transfer zone).

345 The Waikirikiri River has its headwaters in the foothills of the Southern alps and receives  
346 considerably less runoff than the other rivers. The 1 km long study reach is situated near  
347 Hororata where the river leaves the foothills and crosses the western margin of the  
348 Canterbury Plain. A long-term (58 years) flow monitoring site located upstream of the study  
349 reach at Whitecliffs shows a mean annual flow of  $4.5 \text{ m}^3 \cdot \text{s}^{-1}$ , and peak annual flow of  $28$   
350  $\text{m}^3 \cdot \text{s}^{-1}$ . The Waikirikiri River is also the least “flashy” with an average of only one event each  
351 year exceeding a flow of three times the median flow. As a result of its lower flow and high  
352 transmission losses, the Waikirikiri River is subject to intermittent flow within our study  
353 reach (Larned et al., 2008; Di Ciacca et al., 2023). The Waikirikiri study reach is naturally  
354 incised between Pleistocene terraces, with no engineered flood controls. The active  
355 braidplain, which typically has 1-2 braids, can freely adjust between these contemporary  
356 braidplain margins, however, relatively dense exotic vegetation covers much of the  
357 contemporary braidplain.

358



359 **Table 1.** Characteristics of the three study catchments. Mean values are given unless stated  
 360 otherwise. FRE3 is the annual number of events exceeding three times the median flow. Bed  
 361 material grain size is near surface but excludes the armour.

	<b>Ngaruroro</b>	<b>Wairau</b>	<b>Waikirikiri</b>
Study reach length (m)	3000	2200	1000
Contemporary braidplain width in study reach (m)	300	400	460
Active braidplain width in study reach (m)	300	400	55
Braiding index in study reach	2.95	1.96	1.56
Reach slope ( $m.m^{-1}$ )	0.003	0.003	0.006
Catchment Area ( $km^2$ )	1930	3320	250
Catchment rainfall ( $mm.y^{-1}$ )	1414	1543	1045
Catchment potential evapotranspiration ( $mm.y^{-1}$ )	722	693	750
Annual low flow ( $m^3.s^{-1}$ )	1.2	9.9	0.97
Median flow ( $m^3.s^{-1}$ )	23.1	61	2.35
Mean flow ( $m^3.s^{-1}$ )	40	100	4.5
Annual peak flow ( $m^3.s^{-1}$ )	1546	1911	28.3
FRE3	6.1	10.7	1.1
River loss at study reach ( $m^3.s^{-1}.km^{-1}$ )	~0.6	≥0.2	0.25-0.65

362  
 363 All three rivers share a similar bedload lithology dominated by Jurassic greywacke. In the  
 364 study reaches, the Ngaruroro is bounded to the north by Pliocene siltstone and limestone  
 365 (Lee et al. 2011), while the Wairau is bounded to the north by schist (Begg and Johnston  
 366 2000). These two rivers lose water southwards, the river losing reaches being the primary  
 367 source of recharge for the alluvial aquifers hosted by Holocene gravels. In the Waikirikiri  
 368 study reach, the river is bounded by Pleistocene glacial outwash gravels (Forsyth et al.  
 369 2008). These gravels form the surface expression of a large, stratified aquifer system hosted  
 370 by a composite of alluvial fans which underlies the Canterbury Plains. The Ngaruroro and  
 371 Waikirikiri study reaches are both situated close to the apex of the river system's alluvial fan  
 372 (close to where the rivers emerge from the foothills).

373

374 Both the Wairau and Ngaruroro are affected by gravel extraction, which has lowered the  
375 mean active braidplain bed elevation in the river recharge reaches by approximately one  
376 metre since the 1980's (Gardner and Sharma 2016, Measures 2012). The varying physical  
377 environments, flow regimes, bed adjustment trajectories, and degree of lateral confinement  
378 result in different rates of bed reworking for each river. In particular, the Waikirikiri reworks  
379 its bed less frequently than the Ngaruroro and Wairau.

380

381 *4.2 Field data collection*

382 Investigations in the study reaches involved the collection of a variety of data types (Table  
383 2). Each method and data type has advantages and disadvantages and is scale and process  
384 dependant (Gonzalez-Pinzon et al., 2015; Brunner et al., 2017). Stage and temperature  
385 recorders were established in the study reaches but were difficult to maintain due to  
386 repeated destruction by flood flows and frequent bed movement in the study reaches. Flow  
387 rating was conducted at the top of the reach for the Waikirikiri River, and permanent rated  
388 flow sites located downstream were used for the Ngaruroro and Wairau. A series of flow  
389 loss gauging surveys were undertaken at multiple transects within all three study reaches  
390 across a range of discharges to estimate transmission losses. Due to the difficulty of  
391 measuring flow in the larger rivers (and the related large measurement uncertainty), the  
392 most comprehensive set of flow loss surveys was conducted on the Waikirikiri (Di Ciacca et  
393 al., 2023).

394

395 Table 2. Type and number of measurements undertaken in the three study reaches.

Measurement type	Ngaruroro	Wairau	Waikirikiri
------------------	-----------	--------	-------------

Differential flow gauging	2	2	14
Local river stage/temperature		3	6
LiDAR and bathy surveys	1	2	2
Piezometers	19	31	43
Cored holes	10	8	21
Particle size distribution	36	38	60
Core porosity	6	12	5
Field porosity	3	10	4
Radon-222 samples	5	53	61
tTEM	Y	Y	Y
DualEM	Y	Y	Y
SkyTEM	Y		
ERT surveys		9	11
Ground penetrating radar (GPR)			5
DTS installations (vertical)		2	3
DTS installations (horizontal)			2

396

397 LiDAR data were captured in dry areas of riverbed using a LiDARUSA Snoopy LiDAR scanner  
398 deployed on either a UAV or backpack. Bathymetry and water surface elevation were  
399 mapped using a kayak or remote controlled jetboat equipped with a paired RTK GPS and  
400 echosounder, and wading with an RTK GPS. Interpolation, or (where necessary) optical-  
401 bathymetry techniques, were used generate high-resolution bathymetry maps from less-  
402 dense echosounder survey data. The dry topography from LiDAR was stitched together with  
403 the bathymetry data to provide a complete digital elevation model (DEM) for each reach at  
404 a spatial resolution of 1 m or less, and a vertical accuracy of  $\pm 0.1$  m in dry areas and  $\pm 0.2$  m  
405 in wet areas.

406 Piezometers were installed at different depths to provide a time series of water levels and  
407 temperature, and to enable sampling for radon-222 analysis. The piezometers were  
408 installed with 50mm diameter PVC. Screens were a 1-2m length of slotted casing with a  
409 geotextile sock and sand pack around the screen, and cement grout around the overlying  
410 casing. A sump was used to collect downward percolating water in situations where pore  
411 water pressure was below saturation. Drilling methods involved a mix of rotary and sonic

412 drilling, the former being used to install the piezometer network. Sonic drilling with a  
413 Geoprobe 8140LC (76.2mm diameter core) was conducted to collect cores for detailed  
414 logging and sediment analysis (grainsize and porosity). The sonic drilling method is not ideal  
415 as it can be difficult to get good core recovery, particularly in coarser or loose near-surface  
416 sediments. As a result, the core record is incomplete, however, there is currently no better  
417 method available to extract several meters of core from coarse riverbed deposits. Because  
418 core recovery was variable, data from individual drillholes were fragmented, and sediment  
419 analysis was only conducted on the most intact cores (0.1-1.2 m in length), with samples  
420 taken for grainsize and porosity analysis. Near-surface bed material grain size distribution  
421 and porosity were measured using manual excavation sieving combined with a detailed  
422 photogrammetry method to calculate excavation volume (Montgomery et al. *subm.*).  
423 Particle size distribution was characterised by fitting Gompertz and Weibull curves (Bayat et  
424 al. 2015) to the sieved sediment data, and summary statistics determined via the method of  
425 Folk and Ward (1957).

426 The base of the BPA was identified in two ways. The first method was by mapping surface  
427 morphology, since the deepest areas of pools represent the scouring depth that has  
428 occurred during flooding. Surface and bed morphology was captured using remote sensing  
429 (photogrammetry, LiDAR, and bathymetry). The second method was through observations  
430 in drill core with good core recovery, where sediments beneath the BPA are characterised  
431 by more cohesion and a finer matrix. To enable data to be compared, contacts between the  
432 braidplain gravels and underlying sediments (depositional unconformity) have been  
433 expressed as depth below a detrended surface representing cross-section mean  
434 contemporary braidplain surface elevation. This datum was chosen because of the spatially  
435 variable and temporally dynamic river bed levels.

436 Hydrogeophysical methods were also used to image the subsurface, including passive (DTS)  
437 and active (ADTS) distributed temperature sensing (Banks et al., 2022), ground penetrating  
438 radar (GPR), electrical resistivity tomography (ERT), transient electromagnetic (tTEM) and  
439 electromagnetic induction (DualEM421). The tracks prepared for tTEM and DualEM surveys  
440 are evident in the aerial photos shown in Figure 3. SkyTEM data were also available for the  
441 Ngaruroro area (Rawlinson et al. 2021). Of the hydrogeophysical methods employed,  
442 DTS/ADTS, and ERT were the most successful methods for delineating sediment structure  
443 and saturation associated with the river. The resistivity of New Zealand braided river water  
444 (fluid specific conductance  $\sim 5 \text{ mS}\cdot\text{m}^{-1}$ ) and associated gravel deposits is very high (400-  
445 10,000  $\Omega\text{m}$ ). For this reason, we think there was insufficient resistivity contrast for  
446 electromagnetic and ERT methods to reveal distinct subsurface features in most of our  
447 surveys. SkyTEM data did provide good definition of the basement contact beneath the  
448 Ngaruroro River but did not reveal any clear structural features in the near surface (<10 m).  
449 GPR surveys that were trialled at the Waikirikiri site clearly revealed the shallow water table  
450 but did not reveal any clear structure beneath the water table due to reflection of the  
451 signal.

452 Samples for radon-222 analysis were collected in 250 ml bottles in the Waikirikiri (Songola  
453 2022) and Wairau reaches from riffles, at different depths in pools, and from purged  
454 piezometers. Samples were analysed 21-100 hours after sampling for Waikirikiri, and 20-24  
455 hours for the Wairau. Laboratory analysis for radon activity was conducted with a RAD7  
456 (Durrige 2020a), RAD H2O (Durrige 2020b), and active DRYSTIK (Durrige 2021) in a  
457 closed loop system, with the results adjusted for decay since the time of sampling (WAT250  
458 method). The radon activity and uncertainty values reported here follow the approach of  
459 Durejka et al. (2019), with the mean and standard deviation calculated from five counting

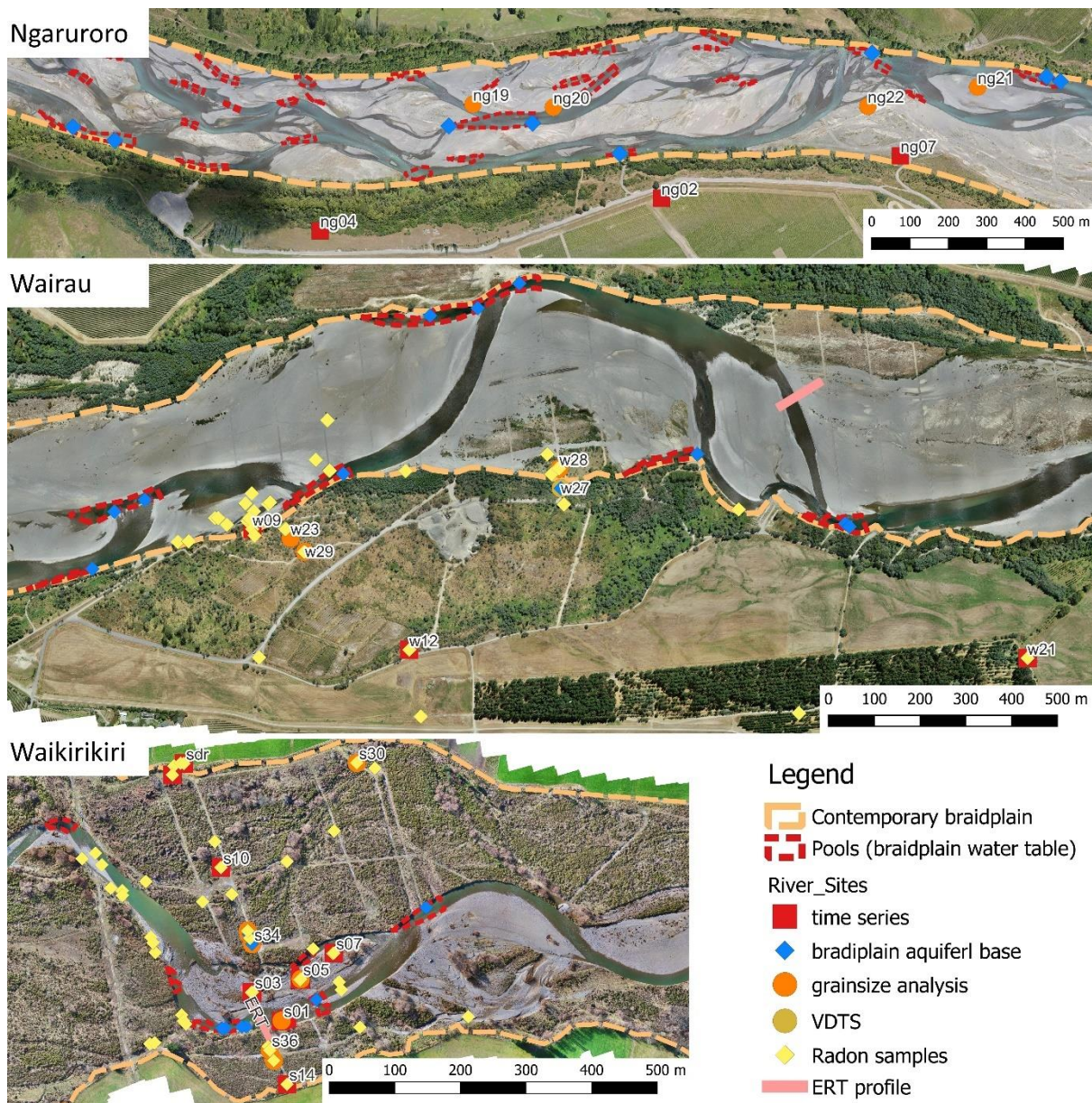
460 cycles, with duplicate samples pooled (ten cycles total). Additional radon measurements  
461 were made in the field using the RAD AQUA method (DurrIDGE 2020c) to verify the WAT250  
462 method results, and these returned similar values. For this study we have reported the  
463 WAT250 data, which has a larger uncertainty associated with the measurements but  
464 enables more samples to be collected in a short time frame from remote field sites. To  
465 reduce the uncertainty of the WAT250 results, we increased the aeration time to 10  
466 minutes, and the analysis duration recommended in the DurrIDGE manual to 5 cycles of 10  
467 minutes.

468

## 469 **5.0 Field observations**

470 A hydraulically disconnected river-regional aquifer system has been identified from drilling  
471 and monitoring data in the Waikirikiri study reach (Banks et al. 2022, Di Ciacca et al. 2023),  
472 and at the upper part of the Ngaruroro study reach. A hydraulically connected river-regional  
473 aquifer system is observed in the Wairau study reach, and in the lower part of the  
474 Ngaruroro study reach. Evidence for the proposed conceptualisation is provided below  
475 based on data type. Data referred to in the text and figures is shown spatially in Figure 3.  
476 Points where the base of the BPA has been observed in cores, or inferred via deep pools are  
477 identified.

478



479

480 **Figure 3.** Data sources referred to in the text.

481

482 *5.1 Geology and geomorphology*

483 The BPA lateral extent in our three sites is identified geomorphologically as being at the  
 484 contemporary braidplain margins (orange dashed lines in Figure 3). The contemporary  
 485 braidplain margins in our study reaches are either artificially confined by rock armouring or  
 486 willow planting for flood protection (Wairau and Ngaruroro), or by terrace boundaries  
 487 (Waikirikiri). These relatively static lateral controls result in the abutment of relatively loose

488 (recently active) braidplain gravels against older, more poorly sorted sediments. In the  
489 Wairau and Ngaruroro rivers the artificial lateral controls are sufficiently narrow that the  
490 entire contemporary braidplain is regularly reworked (i.e., the active braidplain margins and  
491 contemporary braidplain margins are essentially the same). In the Waikirikiri, the active  
492 braidplain is narrower than the contemporary braidplain and the active braidplain is able to  
493 adjust laterally, reworking the contemporary braidplain gravels.

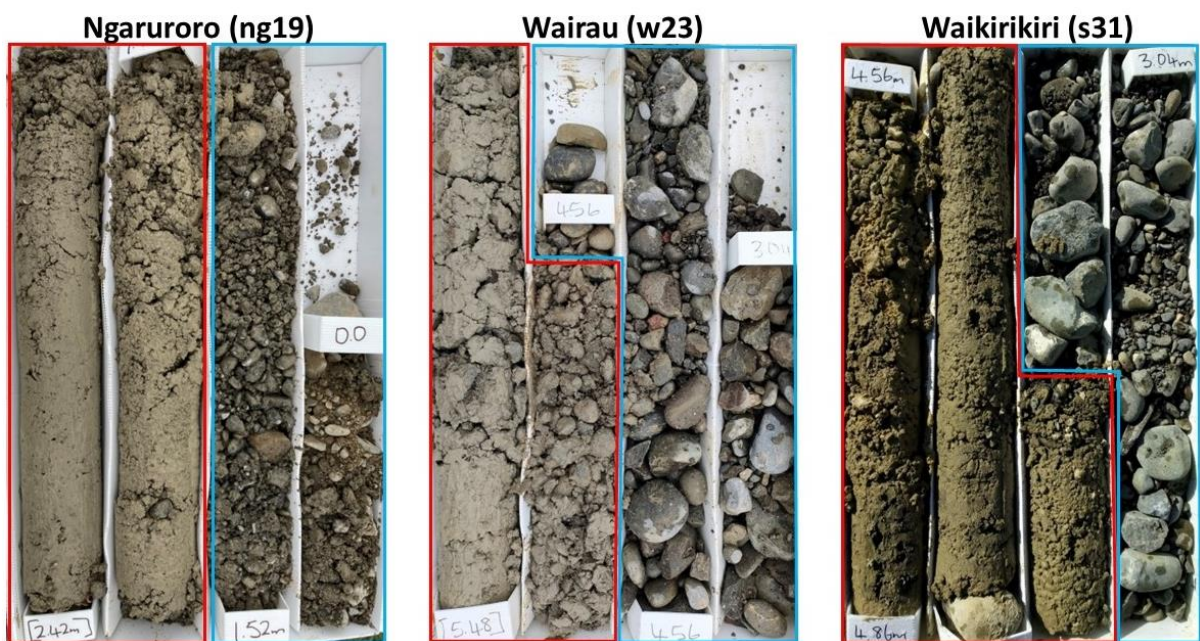
494 In all three braided rivers, deep pools form at the toe of riffles. In the Wairau and  
495 Ngaruroro, these are amplified at the braidplain margins where river flow is reflected by  
496 rock armouring or willow plantings that limit lateral erosion and enhance bed scour. These  
497 pools are zones where the BPA discharges to the river. Parafluvial seeps are commonly  
498 observed in these locations, which have higher radon-222 activities and summer  
499 temperatures that are cooler than adjacent river braids. The surface expression of the BPA  
500 can be seen in abandoned channels where the braidplain surface topography drops below  
501 the braidplain water table and exposes groundwater (static pools or flowing springs). These  
502 areas are demarked by dashed red lines in Figure 3.

503 The depositional unconformity at the BPA base in recovered cores was observed at 1.7-2.0  
504 m depth beneath the mean bed level of the contemporary braidplain in the Ngaruroro study  
505 reach, 4.3-5.0 m depth in the Wairau, and 2.1-3.7 m depth in the Waikirikiri. The greater  
506 depth in the Wairau River is unsurprising, as this river has the highest flood flows and is  
507 tightly confined by engineering works, resulting in greater depths of bed reworking.

508 At the Waikirikiri site, the contact of the depositional unconformity was seen as a change  
509 from grey-brown postglacial sandy gravels to yellow-brown clay-rich glacial outwash gravels  
510 (Figure 4). During drilling and completion of the groundwater monitoring wells, a drop in the  
511 water level with depth below the glacial contact was observed. Six cores were drilled just



512 beneath the unconformity at various locations within the contemporary braidplain margins  
 513 to investigate the saturation status beneath the braidplain gravels. These holes were drilled  
 514 through the low permeability contact layer until an apparent increase in permeability was  
 515 encountered, at which point the water level in the drillhole dropped significantly.  
 516 Piezometers screened beneath the base of the BPA and above the regional water table  
 517 showed low and unvarying water levels, indicating unsaturated or variably saturated  
 518 conditions (Figure 7). Our explanation for the presence of this variably saturated zone is that  
 519 the glacial outwash gravels are stratified, and vertical infiltration to the regional aquifer is  
 520 limited by the lower permeability horizons of silt and clay. The presence of higher  
 521 permeability horizons within the stratified postglacial sequence allows water to move  
 522 laterally away from the recharge zone at a rate that exceeds vertical infiltration, enabling  
 523 unsaturated or variably saturated conditions to form.  
 524



525  
 526 **Figure 4.** Representative core samples across the unconformity at the three study sites  
 527 (blue=braidplain gravels, red=underlying very poorly sorted consolidated gravels)

528

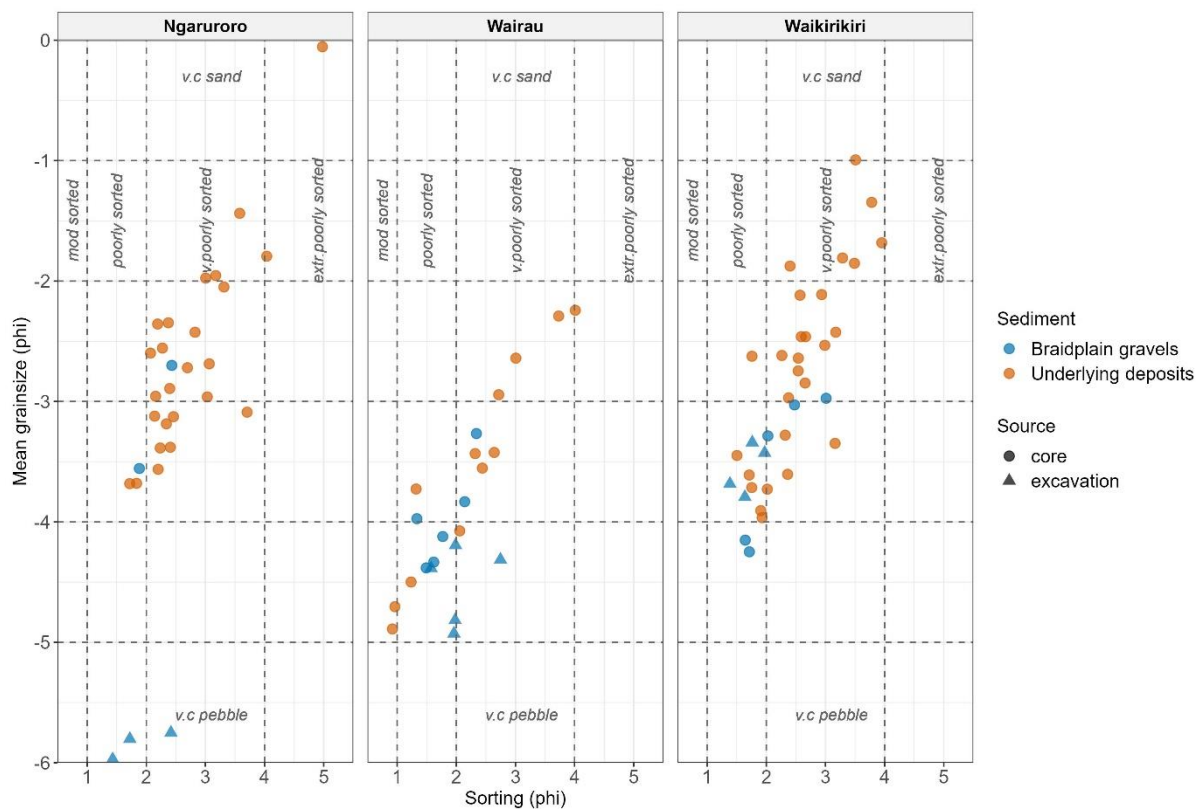
529 At the Wairau River study site, the base of the BPA is visible as a change from grey-brown  
530 sandy clast supported gravel to more cohesive and poorly sorted gravel with increasing  
531 proportions of silt and clay. Just beneath this unconformity is a more prominent contact  
532 with yellow brown silty clay-bound gravel associated with old outwash fan deposits along  
533 the Richmond Range (not shown in Figure 4, but evident in Figure 10). Note that some of  
534 the Wairau core holes were positioned on the berms (outside of what we are referring to as  
535 the contemporary braidplain), where the active braidplain was located prior to river re-  
536 alignment in the 1960s. The river can no longer mobilise sediments on these berms due to  
537 rock armouring of the banks leaving a recent remnant braidplain gravel deposit beneath the  
538 southern berm. This deposit is both spatially and vertically separate from the contemporary  
539 braidplain (the mean bed level of the contemporary braidplain is approximately 2m below  
540 the berms).

541 In the Ngaruroro study site, the unconformity at base of the BPA is more gradational,  
542 manifesting as an increase in silt and clay content between 1.7 and 2.0 m depth visible  
543 within bore logs (Figure 4) and particle size distribution (Figure 5). As with the Waikirikiri  
544 River, a drop in the water table was observed while drilling beneath this lower permeability  
545 unconformity. The less-distinct base to the BPA in the Ngaruroro study reach is likely  
546 because the reach is depositional, so the underlying gravels were deposited relatively  
547 recently compared to the other study reaches.

548 Particle size distribution summary statistics of core samples collected by sonic drilling and  
549 bed excavation are shown in Figure 5, with classifications according to the Folk and Ward  
550 (1957) scale. A relationship between sorting and grainsize is apparent at each site, with  
551 poorer sorting corresponding to an increase in the finer fraction. Shallow braidplain gravels

552 are overall poorly sorted (1-2, data mean: Ngaruroro 1.98, Wairau 1.90, Waikirikiri 1.96),  
 553 whereas the underlying gravels tend to be very poorly sorted (2-4, data mean: Ngaruroro  
 554 2.88, Wairau 2.28, Waikirikiri 2.60). The grainsize of the braidplain gravels is generally  
 555 coarser (mean: Ngaruroro -4.76, Wairau -4.23, Waikirikiri -3.55) than the underlying very  
 556 poorly sorted sediments (mean: Ngaruroro -1.64, Wairau -3.54, Waikirikiri -2.69).

557



558

559 **Figure 5.** Grainsize analyses and sorting indices from samples beneath the three study  
 560 reaches. Dashed lines are breaks for grainsize and sorting indices (after Folk and Ward  
 561 1957).

562 Core recovery at all sites was typically poor in the contemporary braidplain gravels, which  
 563 mostly consist of loose gravel and cobbles, with a high proportion of sand but only a trace of  
 564 silt and clay. Because of this, some of the braidplain gravel samples have been sourced from  
 565 samples manually excavated from the braidplain subsurface (Figure 5). These excavated

566 samples exclude the surface armour common in gravel bed rivers. For the Wairau data set  
567 there is no clear separation in the particle size distribution between braidplain and  
568 underlying gravels. Wairau sediments are coarser than the other two sites, because of the  
569 high-energy of this river system. The coarseness of the sediments greatly hampers core  
570 recovery, so it is possible that the lack of separation is an artefact of the loss of finer  
571 fractions in some samples during drilling.

572

### 573 *5.2 LiDAR and bathymetry*

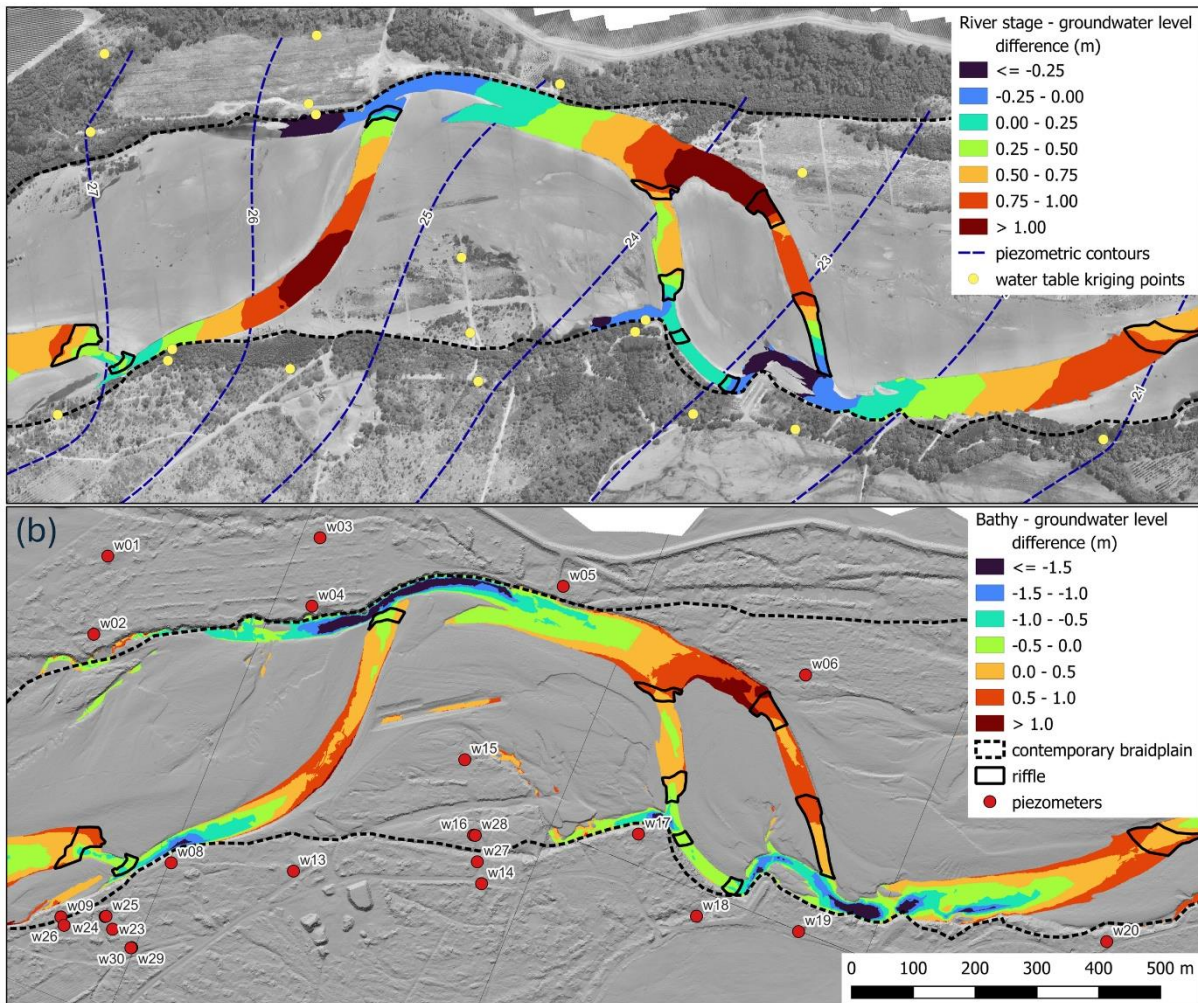
574 LiDAR and bathymetry surveys were conducted in each study area to understand the  
575 spatially varying relationship between the river surface, bed levels, and water levels in the  
576 braidplain and regional aquifers. Repeat surveys were conducted following significant flood  
577 events to capture changes in bed levels. An example of our LiDAR and bed elevation data for  
578 the Wairau River is shown in Figure 6. These data were captured on 19 Feb 2020 at  
579 relatively low flow conditions, measured at  $13.4 \text{ m}^3 \cdot \text{s}^{-1}$  to  $11.5 \text{ m}^3 \cdot \text{s}^{-1}$  ( $\pm 3 \%$ ) at the upstream  
580 (left) and downstream (right) margins of Figure 6 respectively. The river water surface and  
581 bed elevation data within the wetted channel are shown on Figure 6 in relation to a  
582 modelled surface of hydraulic head across the river system, represented by piezometric  
583 contours which are shown in Figure 6a. This surface was fitted (sum squared error of  $5 \times 10^{-6}$ )  
584 <sup>6)</sup> to 25 water level observations (yellow points in Fig 6a) located within and outside of the  
585 contemporary braidplain by universal kriging with an exponential variogram of anisotropy of  
586 0.9 at  $090^\circ$ , partial sill 0.31 m, and range 670 m. With such a large variogram range, the  
587 surface should be considered as indicative of an averaged hydraulic head across the regional  
588 and braidplain aquifers. The kriged surface does reveal an inflection of the piezometric  
589 contours across the contemporary braidplain margins, indicating that flow within the BPA is

590 largely controlled by river exchange and preferential flow within the BPA, with flow being  
591 approximately sub-parallel to the contemporary braidplain longitudinal orientation.

592 Fig. 6a reveals locations in the river system where the river water surface is higher than the  
593 braidplain water table (red and orange zones), indicating that the river is losing flow to the  
594 BPA in these areas. Areas of the river which are coloured blue in Fig. 6a represent the  
595 surface expression of the braidplain water table in pools. These are locations where the  
596 river can potentially gain flow. The black areas denoted as “riffles” are identified from a  
597 slope raster derived from the digital elevation model (DEM). Locations where maximum  
598 potential river water loss occurs can be identified in most cases as being situated at the  
599 upstream margins of high elevation riffles.

600 The bathymetry DEM (Fig. 6b) reveals the presence of scouring along the contemporary  
601 braidplain margins, which in the case of the Wairau River is promoted by excessive river  
602 narrowing and rock training banks. The corollary of this scouring is the relative mounding of  
603 gravel in the middle of the contemporary braidplain. The difference between the river bed  
604 level and hydraulic head reveals locations where the river bed is above the braidplain  
605 aquifer, and the river braid has the potential to be losing-disconnected at these locations. In  
606 most cases these areas also correspond to the upstream margins of high elevation riffles.





607

608 **Figure 6.** Images of the wetted Wairau River channel showing differences between (a) river  
 609 water surface and a kriged hydraulic head (overlain on aerial imagery), and (b) bathymetry  
 610 and kriged hydraulic head (overlain on the DEM). River flow is from left to right.

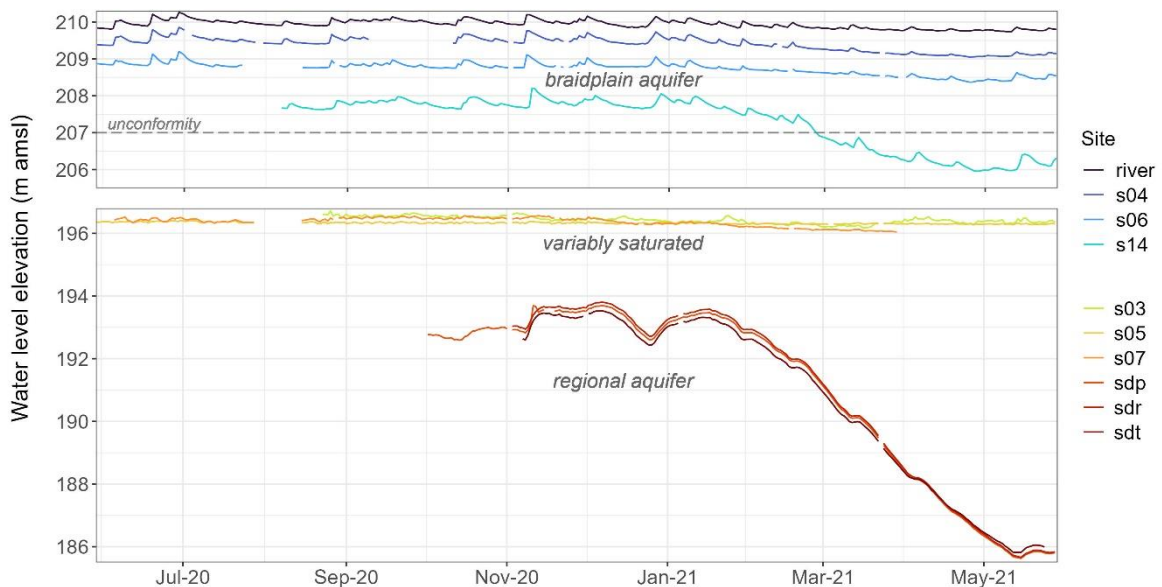
611

### 612 5.3 Water levels and temperature monitoring

613 Hydraulic heads within the braidplain aquifer are dynamic and fluctuate in response to  
 614 changes in river stage. Figure 7 shows heads for the Waikirikiri field site, where the base of  
 615 the BPA is at approximately 207m elevation, and the regional water table is >13m below the  
 616 unconformity. The variably saturated zone (pore water pressure below saturation) is at least  
 617 10m thick. For a river system that is hydraulically connected to the regional aquifer, the  
 618 pressure response outside of the BPA is also dynamic and shows a similar response to the

619 BPA (Figure 7). For a river system with a hydraulic disconnection, the variably saturated  
 620 zone attenuates the pressure fluctuations in the regional aquifer (Figure 7). The relative  
 621 water level depth and hydraulic response in the regional aquifer can therefore provide a  
 622 useful test for hydraulic connectivity between the two aquifer systems.

623



624

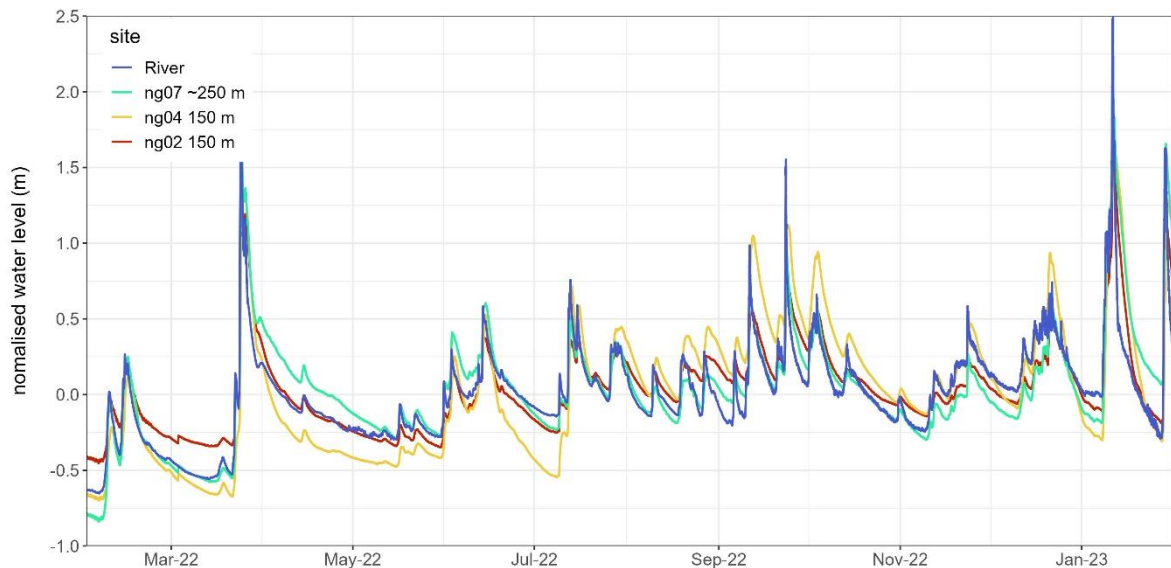
625 **Figure 7.** Water level time series data for the Waikirikiri River and braidplain and regional  
 626 aquifers. Note the vertical offset in the two graphs is due to the thick variably saturated  
 627 zone beneath the braidplain and regional aquifer. Site locations are shown in Figure 3.

628

629 Data from the Ngaruroro reach show characteristics of a regional aquifer that is both  
 630 hydraulically connected to the BPA and either disconnected or transitional (Figure 8). These  
 631 data have been normalised by the median water level to highlight relative changes in  
 632 response. The BPA site (ng07) responds similarly to the river stage but has a slower  
 633 recession rate due to storage in the gravels. The two sites that are screened in the regional  
 634 aquifer (ng02, ng04) are both located 150 m adjacent to and downgradient of the  
 635 contemporary braidplain (see Figure 3). The upstream site, ng04, has the most rapid

636 recession rate and its peak response is slightly delayed compared to ng02 which responds  
637 similarly to the river channel stage. This suggests that this upstream section of the study  
638 reach may be hydraulically disconnected or transitional from the regional aquifer (assuming  
639 similar hydraulic properties throughout the regional aquifer). The water levels in ng04 are  
640 up to 2.4 m below the BPA base (mean 1.8 m) assuming a BPA thickness of 1.6 m below  
641 mean river bed level at this site. During flood flow events, the regional aquifer water level at  
642 ng04 does rise above the river bed elevation, indicating saturated conditions do temporarily  
643 occur during flooding.

644



645

646 **Figure 8.** Normalised water level time series data for the Ngaruroro River, braidplain (ng07)  
647 and regional aquifers (ng02, ng04). Site locations are shown in Figure 3. Distances in the  
648 legend indicate the down gradient distance from the nearest active river channel.

649

650 Figure 9 shows daily average temperatures from representative hydrological settings in each  
651 study reach, and the lateral distance downgradient of the nearest active river channel. For  
652 sites located within the BPA, temperature responses are similar to the river channel, and



653 driven by individual flow events (ng07, w09, s06). However, event-driven responses can be  
654 attenuated, and the season response delayed, at large distances from a channel (s25). Note  
655 also that s06 becomes more responsive after a flood event on 30 May 2021 which has  
656 changed connectivity between the river and groundwater in this piezometer.

657 For sites within the regional aquifer (ng02, ng04, w12, w21, sdg), the event-driven response  
658 is difficult to detect, and the seasonal response depends on the hydraulic relationship  
659 between the braidplain and regional aquifers. Sites ng02 and ng04 are equidistant from the  
660 Ngaruroro BPA, however ng04 is in a position where the base of the braidplain gravels and  
661 regional water table are approximately 1.8m apart, potentially with an intervening variably  
662 saturated zone, whereas at ng02 the braidplain and regional aquifers are hydraulically  
663 connected. This difference in hydrologic condition may explain the delayed seasonal  
664 response in ng04. In the Waikirikiri system, the variably saturated zone is considerably  
665 thicker (about 12m), which almost completely attenuates the seasonal temperature  
666 response in the regional aquifer.



667

668 **Figure 9.** Representative temperature time series for the three study sites. Piezometer

669 locations are shown in Figure 3, sites ng07, w09, s06 and s25 are screened in the BPA.

670

671 In the Waikirikiri and Ngaruroro river systems, the temperature signals propagate efficiently

672 from river channels to the BPA compared to the regional aquifer. This highlights the

673 distinction between these two aquifers, with the BPA acting as an intermediary in

674 groundwater – surface water exchanges.

675

#### 676 *5.4 Radon-222 sampling*

677 A summary of the radon-222 results and measurement uncertainties for surface water and

678 groundwater sources in the Wairau and Waikirikiri reaches is shown in Table 3. In the

679 Wairau system, samples from riverbed piezometers and riverbed seepages have similar

680 radon activities with ranges 1724-2849 BQ.m<sup>-3</sup> and 368-2585 BQ.m<sup>-3</sup> respectively.

681 Accordingly, samples from seepages and riverbed piezometers are both considered to  
 682 represent the braidplain aquifer.

683 The radon data show distinct groupings, with radon-222 activities increasing from river  
 684 channel to BPA to regional aquifer. At both sites, radon activities in river run samples were  
 685 significantly lower than those in BPA samples. In the Wairau study reach, there is a notable  
 686 overlap in radon activities between the braidplain and regional aquifers, indicating a likely  
 687 hydraulic connection between these two systems. Conversely, in the Waikirikiri study reach,  
 688 there is a downward increase in radon activities from the BPA to the variably saturated zone  
 689 and further into the regional aquifer, with no overlapping values. This suggests a hydraulic  
 690 disconnection between the BPA and the regional aquifer in the Waikirikiri reach.

691

692 **Table 3.** Measured radon-222 activities and one standard deviation uncertainties (BQ.m<sup>-3</sup>)  
 693 for the Wairau and Waikirikiri study reaches.

River	Wairau			Waikirikiri			
	River run	Braidplain aquifer	Regional aquifer	River run	Braidplain aquifer	Variably saturated glacial outwash sediments	Regional aquifer
Samples	14	11	21	10	38	7	6
Rn min	260 ± 85	368 ± 150	739 ± 272	384 ± 185	1791 ± 481	7017 ± 3607	16111 ± 3305
Rn max	604 ± 224	2849 ± 826	5700 ± 629	809 ± 443	9545 ± 1378	14654 ± 4338	22655 ± 2221
Rn mean	395 ± 180	1307 ± 361	3263 ± 666	568 ± 356	4569 ± 1002	11814 ± 2589	19184 ± 2763

694

695 The determination of residence times between the river and each aquifer depends on  
 696 knowing the initial channel condition, representative secular equilibrium for the host gravel  
 697 deposit, as well as a well-defined flow path length. Our estimate of the initial river channel  
 698 condition is 260 BQ.m<sup>-3</sup> for Wairau and 380 BQ.m<sup>-3</sup> for Waikirikiri, reflecting the lowest  
 699 measured river radon-222 activities. A secular equilibrium estimate of 5000 BQ.m<sup>-3</sup> was  
 700 derived for Wairau aquifer samples by plotting measured groundwater radon activity

701 against distance of the piezometer from the river and fitting the ingrowth equation to the  
702 data to determine the 21 day equilibrium value. This exercise indicated that the Wairau BPA  
703 activities are too low for samples to reach equilibrium. In the absence of sediment specific  
704 data, the Wairau aquifer secular equilibrium was chosen to represent the Wairau BPA  
705 equilibrium. The secular equilibrium for the Waikirikiri BPA is estimated at approximately  
706 8500 BQ.m<sup>-3</sup> based on the lowest activity observed in porewater samples from piezometer  
707 sumps in the variably saturated glacial outwash gravels beneath the braidplain aquifer (7017  
708 BQ.m<sup>-3</sup>), and the highest activity observed in the BPA (9545 BQ.m<sup>-3</sup>). Based on the secular  
709 equilibrium values chosen, residence times for our study reach samples are estimated to be  
710 in the range of 0.1 to 4.4 days for the Wairau BPA in the study reach and 1 to >12 days for  
711 the Waikirikiri BPA. Due to the large uncertainties associated with the WAT250 method,  
712 these estimates should be considered for comparative purposes only.

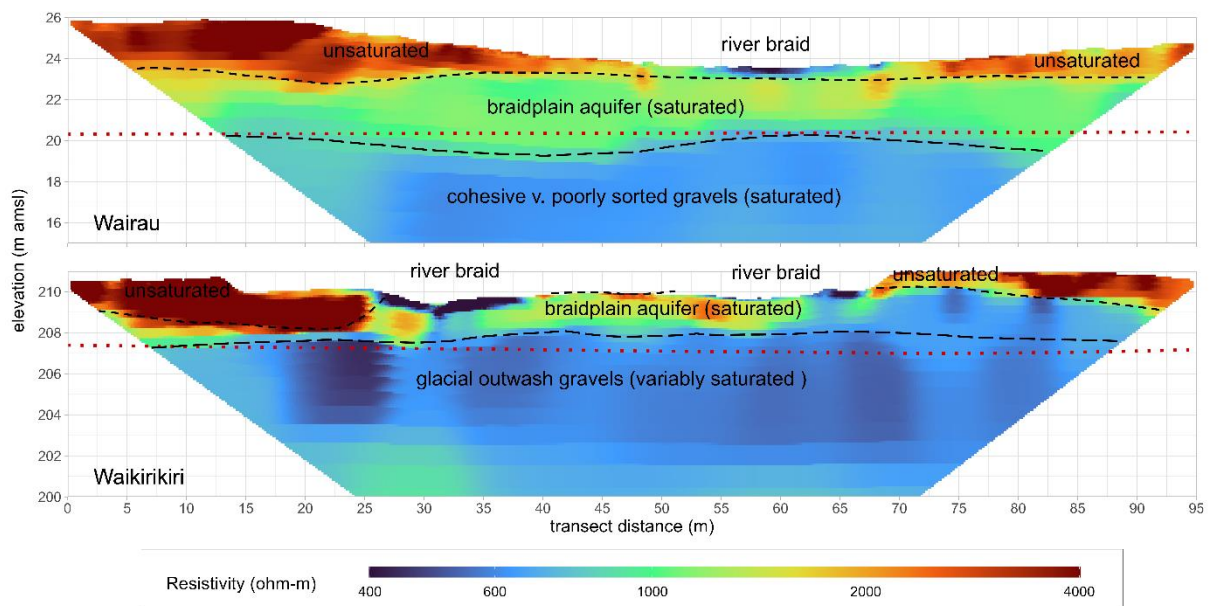
713

#### 714 *5.5 Geophysics*

715 ERT surveys of the contemporary braidplain in the Wairau and Waikirikiri reaches yielded  
716 varying degrees of success. The surveys that returned the most consistent subsurface  
717 resistivity response were conducted in the river channel itself, due to the presence of water  
718 in the near surface, which improved the connection between electrodes and the underlying  
719 resistive substrate. Figure 10 shows dipole-dipole array resistivity profiles across a braid of  
720 the Wairau (~ 30 m wide), and two braids of the Waikirikiri (~40 m wide). These profiles  
721 reveal the contact between the braidplain aquifer and underlying sediments (the  
722 unconformities shown in Fig. 4) at elevations consistent with drillhole coring. For  
723 comparison, the elevation of the same unconformity, derived by kriging intercepts of the  
724 BPA base within the contemporary braidplain (Figure 3.), is shown in red in Figure 10. The

725 two profiles are shown at the same spatial and resistivity scale, and an interpretation has  
 726 been made based on drilling information. Both profiles show a contrast between resistive  
 727 (~1000 ohm-m) loose sandy gravels that host the BPA, and the underlying lower resistivity  
 728 (<800 ohm-m) associated with older, very poorly sorted sediments. The Wairau profile  
 729 reveals the unconformity at the base of the active braidplain gravels as a less resistive layer  
 730 at ~19.5 m elevation, and a saturated BPA thickness of ~3.5 m. On the Waikirikiri profile, the  
 731 unconformity at the base of the braidplain gravels lies at ~207.5 m elevation, and the  
 732 saturated thickness of the BPA is only 2-2.5 m. The underlying very poorly sorted glacial  
 733 outwash gravels typically show relatively low resistivities ( $\leq 600$  ohm-m) due to the relative  
 734 abundance of clay-sized sediment, even when not fully saturated.

735



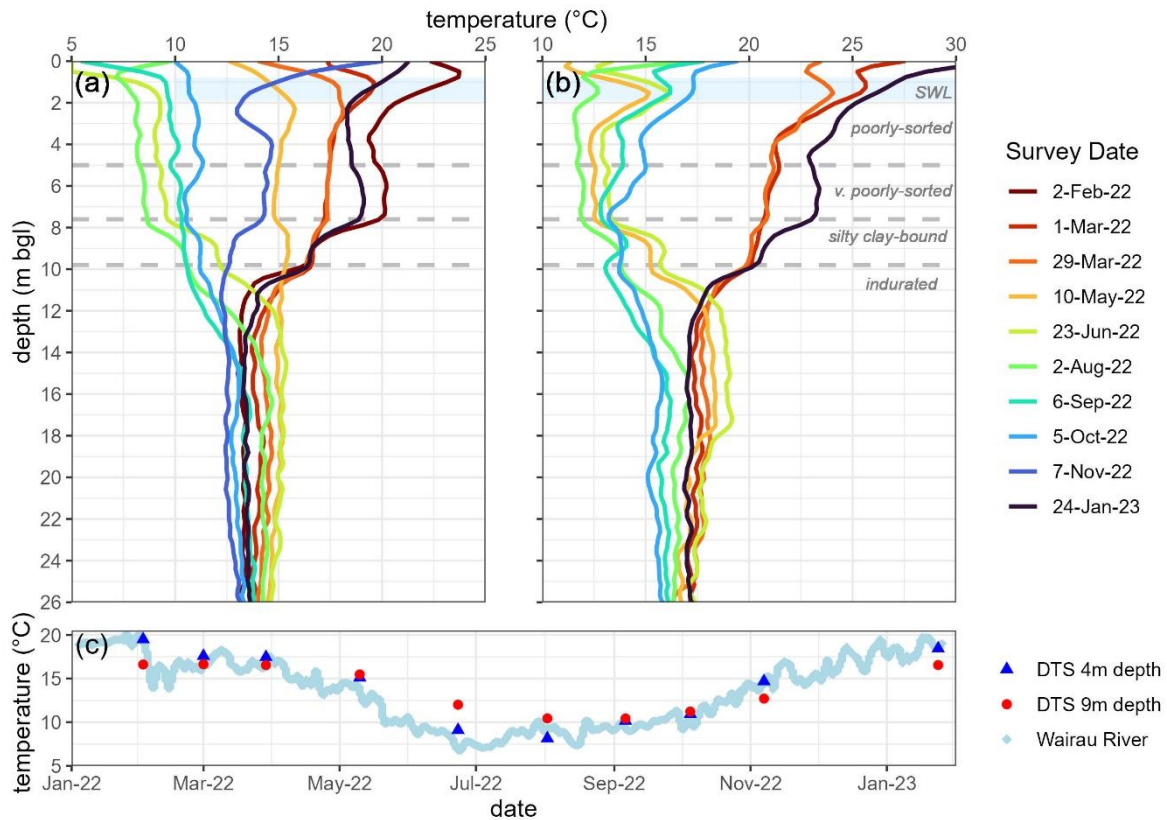
736

737 **Figure 10.** Subsurface resistivity collected by Electrical Resistivity Tomography (ERT) across  
 738 Wairau and Waikirikiri river braids, looking downstream. Surfaces interpreted from the  
 739 resistivity data are shown in black. An interpolated surface for the base of the BPA derived  
 740 from drilling and bed data is shown in red.

741

742 *5.6 Passive and active distributed temperature sensing*

743 The hydrogeologic structure in the Wairau study reach has been assessed by monthly DTS  
744 and ADTS surveys (Figure 11) conducted on a vertically installed fibre optic cable located 20  
745 m from the active braidplain margin (w27 in Figure 3). While w27 lies just outside of the  
746 existing engineered contemporary braidplain, this site does contain remnant braidplain  
747 sediments deposited prior to stabilisation of the river margins in the 1960s. The timing of  
748 the DTS surveys with respect to river temperature is shown in Figure 11c. The survey  
749 temperature profiles show consistent inflections with depth due to the attenuation of the  
750 river recharge temperature response through saturated sediments of contrasting hydraulic  
751 conductivity (Figure 11). These inflections correspond to the depths where a change in  
752 sediment characteristics can be seen in the bore log, manifest as progressively increased  
753 sediment cohesion, poorer sorting, and increasing silt and clay content with depth. In the  
754 DTS profile, the older silty clay-bound and indurated sediments have a large influence on  
755 subsurface flow, i.e., a reduction in flow through this material.



757

758 **Figure 11.** Vertical (a) distributed temperature sensing (DTS) and (b) active-distributed  
 759 temperature sensing (A-DTS) surveys conducted on the south bank of the Wairau River on  
 760 w27. The river temperature over the period of the surveys is shown in (c) along with  
 761 temperatures measured by DTS at 4 and 9 m depth. SWL=static water level measurements  
 762 over the survey period

763

## 764 6.0 Characteristics of the identified braidplain aquifers

765 A summary of the approximate dimensions and potential maximum groundwater storage  
 766 volumes of the three braidplain aquifers investigated is shown in Table 4. In all three  
 767 reaches, the BPA is laterally extensive, but very thin.

768 The Wairau River has the greatest BPA storage potential, largely due to its observed  
 769 saturated thickness of up to 4.1 m. However, the Wairau is also a highly channelised river,  
 770 and has a large bathymetric range, giving its BPA a large potential variability in saturated  
 771 thickness in response to river channel stage fluctuations. Of significance for water  
 772 management in the Wairau Plain is that the very poorly sorted gravels are thin beneath the  
 773 Wairau contemporary braidplain and underlain by buried fans of silty clay-bound and  
 774 indurated gravels which act as a vertical flow barrier (see Figure 10). Gravel extraction from  
 775 the river system has dropped the mean bed level by approximately 1 m within our study  
 776 reach since the early 1990s (Gardner and Sharma, 2016). This has allowed the river to  
 777 rework sediment to greater depths, which has thinned and reduced the effective  
 778 transmissivity of the gravel sequence overlying the buried fan deposits in addition to  
 779 reducing the hydraulic gradient between the river system and regional aquifer.

780

781 **Table 4.** Dimensions and maximum storage volumes of braidplain aquifers observed in the  
 782 three study areas.

River	Approximate width (m)	Contact depth (m) min-max (mean)	Porosity min-max (mean)	Storage volume (m <sup>3</sup> .m <sup>-1</sup> )
Ngaruroro	300	1.2 - 2.4 (1.6) n=4	0.12-0.35 (0.21) n=9	80-150
Wairau	450	2.4– 5.7 (4.1) n=6	0.09-0.46 (0.22) n=21	210-500
Waikirikiri	400	2.0 - 3.7 (2.8) n=16	0.09-0.22 (0.14) n=9	130-240

783

784 **7.0 Discussion**

785 The proposed conceptualisation enables a complex braided river system of high complexity  
 786 to be represented by a few key hydrogeological elements. These are represented in Figure 1  
 787 as a contemporary braidplain, the margins of which mark the lateral extent of the braidplain  
 788 aquifer (1), an underlying unconformity with more consolidated and more poorly sorted



789 sediments (2), and observations of the hydraulic relationship between the braidplain and  
790 regional aquifers (a or b). For braided rivers, this approach integrates existing concepts of an  
791 alluvial aquifer, and hydrological hyporheic and parafluvial zones into a single  
792 conceptualisation of the contemporary braidplain subsurface. By identifying the base and  
793 margins of the BPA, and the process which forms it (reworking of bed material), the vertical  
794 and lateral extents to which hyporheic and parafluvial exchange occur can be identified by a  
795 change in sediment characteristics.

796

797 Point-scale features of braided rivers are described well by the existing hydrological  
798 framework proposed by Fox and Durnford (2003) and modified by Brunner et al. (2009a and  
799 b). Under this framework, individual channels can be considered as hydrologically connected  
800 (gaining or losing), disconnected (losing), or transitional (losing). However, this framework  
801 starts to break down for braided rivers at local to sub-catchment scales, as all four of these  
802 hydrological states can occur along a single cross-section of the braidplain regardless of  
803 whether the river has a net gain or loss. However, at the reach or sub-catchment scale, a  
804 braided river can be considered a *river system*, which can be described by any one of those  
805 hydrological states in relation to the regional groundwater system. For example, a river  
806 braidplain reach can be hydrologically disconnected and be losing water to groundwater  
807 overall, even though individual channels are hydrologically connected and locally gaining  
808 flow from BPA groundwater. The conceptualisation posed by Fox and Durnford (2003) can  
809 therefore be applied to different scales within a braided river system, but its application,  
810 and therefore interpretation of field measurements, requires knowledge of subsurface  
811 structure and saturation.

812

813 The difference in sediment characteristics above and below the unconformity at the base of  
814 the BPA indicates that the process of BPA formation is controlled by the mobilisation of bed  
815 material during flood flows, which loosen and sort the braidplain gravels, and winnow the  
816 finer fraction. This process of gravel mobility associated with flood events is supported by  
817 bathymetric observations of the depth of river channel scouring in deeper pools which  
818 agrees with the depths of the unconformity in core data. In the absence of drill core and  
819 particle size distribution data, we suggest that the elevation of pool depths measured soon  
820 after a flood event can be used to approximate the base of the BPA. This will only provide a  
821 minimum depth of the BPA base since the river is expected to deposit some sediment in  
822 scoured areas during the flow recession. The thickness of a river's BPA is likely to depend on  
823 the inter-relationship between several factors, including contemporary braidplain width,  
824 sediment characteristics and the balance of sediment supply, the frequency and magnitude  
825 of peak flow events, and the use of "hard engineering" to control a river's position. While  
826 some of these factors are natural, the factors related to width and depth are influenced by  
827 river engineering applied at each river. The Wairau River has the thickest BPA and has the  
828 highest hydrological energy of the reaches studied. This river is considered by some river  
829 engineers to be excessively narrowed, and a wider contemporary braidplain may result in a  
830 dispersion of energy during flood flows, and subsequent thinning of the BPA. Interestingly,  
831 the Ngaruroro River is also subject to high peak flows, although bed mobilising flows occur  
832 less frequently than the Wairau. It is likely that the Ngaruroro BPA is being thinned by the  
833 large volume of gravel extraction occurring within the study reach.

834

835 The LiDAR and bathymetric data gathered from our three study sites indicate that individual  
836 river channels locally merge with and diverge from the water table surface of the BPA.

837 Water exchange across the bed is determined by bathymetry and hydraulic properties,  
838 where the river can be forced above the water table by gravel lobes or dropped into the  
839 water table in locations of scouring. Areas of relatively still water (pools) are therefore the  
840 surface expression of the BPA, with seeps representing locations where the bedform drops  
841 below the level of the BPA water table. This explains the occurrence of higher radon-222  
842 activities in pools compared to flowing river channels, as well as differences in seasonal  
843 water temperature.

844

845 For the interpretation of field data, the proposed conceptualisation highlights the  
846 importance of identifying and knowing the nature of the relationship between these three  
847 potential water sources to interpret observations. For example, to understand the nature  
848 and magnitude of river-aquifer interaction by only sampling radon-222 in river channels can  
849 be misleading. This is because the radon activity measured in the river depends both on the  
850 river setting (run or pool), and the nature of the interaction between the BPA and regional  
851 aquifer.

852

853 From a modelling perspective, it is questionable if a streambed conductance term is an  
854 appropriate physical mechanism for representing braided river-aquifer exchange at the local  
855 or catchment scale. The role of bed conductance, if significant, is to regulate exchange  
856 between individual river channels and the BPA. Due to the relatively high transmissivity of  
857 the bed materials, hyporheic exchange is an integral process of braided river flow, and  
858 water can be seen to freely exchange between the surface and the bed. It follows that  
859 consideration of water storage in the bed sediments (BPA) with a conductance term to  
860 impede flow beneath those sediments would be a more appropriate approach for

861 simulating braided rivers at larger scales than to simulate individual channels with bed  
862 conductance.

863

864 The BPA concept resolves vague definitions of “groundwater” in groundwater – surface  
865 water interactions in braided rivers by considering the river as a whole system with an  
866 associated subsurface storage component distinct from the regional groundwater system.  
867 This provides specificity to the concept of a “river corridor” (Harvey and Gooseff, 2015),  
868 where a river comprises not just the river channels, but the surrounding, fluvial deposits,  
869 riparian zones, and floodplains between which hydrologic exchange occurs.

870

871 Braided river systems are spatially and temporally variable, which introduces heterogeneity  
872 both within a BPA, and the adjacent older sediments. This heterogeneity can manifest as  
873 preferential flowpaths, which can influence exchange fluxes at a local scale, as evident in  
874 spatial variability of temperature and radon data. While the BPA consists of high  
875 transmissivity sediments, and can itself be considered a preferential flow path at the  
876 regional scale, the presence of preferential flow within the BPA at the local scale is not  
877 captured by the conceptualisation presented here. We therefore recommend application of  
878 the BPA concept at the regional scale, and to provide a hydrogeological context for local  
879 scale studies. An additional consideration for applying the BPA concept is the volume of  
880 reworked material associated with the river. In braided river environments, the volume of  
881 gravel associated with the BPA is large, and significantly greater than the wetted channel  
882 volume at average flow conditions. However, in some gravel bed rivers, the volume of  
883 sediment mobilised by flooding events could potentially be very thin, and the relevance of

884 these mobile sediments on the exchange between the river and regional groundwater  
885 system will depend on the scale of the study.

886 At the regional scale, the BPA concept is best applied to braided rivers that have stable or  
887 actively degrading beds, or have had some form of bank stabilisation, which is common  
888 where flooding is considered a risk to adjacent land. Stabilisation of river margins serves to  
889 increase the frequency of gravel remobilisation within the active braidplain and prevent  
890 reworking of adjacent bed material that may be part of the historical braidplain. Fine  
891 sediment can percolate through the gravels or be deposited on the surface, and if these  
892 gravels are not subsequently reworked, this can gradually consolidate and potentially clog  
893 the pore spaces, accentuating the difference between contemporary and adjacent historical  
894 braidplain sediments. Narrowing the area of braidplain that is reworked can thereby narrow  
895 the BPA. The conceptualisation may be less appropriate, or the BPA boundaries may be less  
896 distinct, where the contemporary braidplain margins are much wider than the active  
897 braidplain and reworked over longer timeframes. This type of braided river behaviour is  
898 typically seen in mountainous areas with low land use pressure, for example in the Southern  
899 Alps of New Zealand, but would have occurred on lowland plains prior to widespread  
900 engineering of river margins in New Zealand during the 1960s. If river channels can adjust  
901 laterally over a wider area, it is expected that sediments within the contemporary braidplain  
902 will be more heterogeneous, with channels of permeable recently mobilised gravel  
903 intermingled with islands/areas of varying age and permeability. In these cases, the extent  
904 of the BPA beyond the active braidplain across the contemporary braidplain may depend on  
905 the frequency of contemporary braidplain reworking, or the connectivity with the active  
906 braidplain. Similarly, it would be difficult to detect the base of the BPA in situations where  
907 the river bed is rapidly aggrading.

908

## 909 **8.0 Conclusions**

910 By investigating the surface and subsurface sediment and saturation in three study reaches,  
911 we have developed a conceptualisation of how braided rivers exchange water at the local  
912 (reach) and sub-catchment (aquifer) scale. The interaction between the river system and  
913 groundwater can be considered to occur between (a) individual river channels and the BPA  
914 (hyporheic and parafluvial exchange), or (b) the braidplain and regional aquifers. Central to  
915 this conceptualisation is the presence of a braidplain aquifer (BPA), a thin (2-5 m) layer of  
916 loose, poorly sorted gravel which is formed via the process of bed mobilisation during flood-  
917 flows. The base of the BPA can be identified in drill core as an unconformity between poorly  
918 sorted unconsolidated gravels overlying more consolidated very poorly sorted gravels.  
919 Individual river channels can be hydraulically connected, transitional, or disconnected from  
920 the BPA, depending on the relationship between the braidplain water table and bathymetry.  
921 The nature of the hydraulic relationship between the braidplain and regional aquifers can  
922 also be hydraulically connected, transitional, or disconnected, depending on the relationship  
923 between the regional water table and base of the BPA gravels. Approaching the braided  
924 river as a (whole) system (river and BPA combined) enables field data to be interpreted  
925 within the context of its water source.

926

927 From a modelling perspective, the conceptualisation enables rivers to be appropriately  
928 represented at a local scale (river-BPA), or a regional scale (BPA/river system-regional  
929 aquifer), depending on the modelling objective. A parallel investigation not presented here  
930 is focussed on the implementation of the proposed conceptualisation into sub-catchment

931 scale models to quantify how changes in river morphology and BPA storage influence  
932 recharge to the regional groundwater system. A key research gap is to understand the  
933 relationship between BPA dimensions, bathymetry, and river flow dynamics, and this is a  
934 subject for future research.

935

### 936 **Acknowledgements**

937 The authors would like to thank the New Zealand Ministry of Business, Innovation and  
938 Employment for funding this research through the project “Subsurface processes in braided  
939 rivers - hyporheic exchange and leakage to groundwater”. We are also grateful to additional  
940 support from Hawkes Bay Regional Council, Marlborough District Council and Environment  
941 Canterbury. We also acknowledge the contribution of the Hydrogeophysics Group, Aarhus  
942 University who carried out the EM surveys on our rivers, and Christy Songola who did the  
943 radon sampling and analysis at our Selwyn study site. Lastly, we would like to express our  
944 gratitude to the reviewers for their valuable comments, which helped us improve the  
945 quality of this article.

946

### 947 **Financial support**

948 This research has been supported by the Ministry of Business, Innovation and Employment  
949 (grant no. LVLX1901).

950

### 951 **References**

952 Anderson, E.I. (2005) Modeling groundwater–surface water interactions using the Dupuit  
953 approximation. *Advances in Water Resources* 28(4), 315-327.

954 Banks, E.W., Simmons, C.T., Love, A.J., and Shand, P. (2011). Assessing spatial and temporal  
955 connectivity between surface water and groundwater in a regional catchment: Implications  
956 for regional scale water quantity and quality. *Journal of Hydrology*, 404(1-2): p. 30-49,  
957 doi:10.1016/j.jhydrol.2011.04.017.

958 Banks, E.W., Morgan, L.K., Sai Louie, A.J., Dempsey, D., Wilson, S.R. (2022). Active  
959 distributed temperature sensing to assess surface water-groundwater interaction and river  
960 loss in braided river systems. *Journal of Hydrology* 615, 128667,  
961 doi:10.1016/j.jhydrol.2022.128667

962 Barthel, R., Banzhaf, S. (2016). Groundwater and Surface Water Interaction at the Regional-  
963 scale - A Review with Focus on Regional Integrated Models. *Water Resources Management*  
964 30: 1–32, doi:10.1007/s11269-015-1163-z

965 Bayat, H., Rastgo, M., Mansouri Zadeh, M., Vereecken, H. (2015). Particle size distribution  
966 models, their characteristics and fitting capability. *Journal of Hydrology* 529, 872-889,  
967 doi:10.1016/j.jhydrol.2015.08.067

968 Begg, J.G, Johnston, M.R. (compilers) (2000). Geology of the Wellington area. Institute of  
969 Geological & Nuclear Sciences 1:250 000 geological map 10. 1 sheet + 64p. Lower Hutt, New  
970 Zealand. GNS Science.

971 Boano, F., Harvey, J.W., Marion, A. Packman, A.I., Revelli, R., Ridolfi, L., Wörman, A. (2014).  
972 Hyporheic flow and transport processes: Mechanisms, models, and biogeochemical



973 implications. *Reviews of Geophysics* 52: 603–679, doi:10.5194/hess-22-1917-  
974 201810.1002/2012RG000417

975 Boano, F., Revelli, R., Ridolfi, L. (2008). Reduction of the hyporheic zone volume due to the  
976 stream-aquifer interaction. *Geophysical Research Letters* 35: L09401,  
977 doi:10.1029/2008GL033554.

978 Booker, D. J. (2013). Spatial and temporal patterns in the frequency of events exceeding  
979 three times the median flow (FRE3) across New Zealand. *Journal of Hydrology (NZ)* 52, 15-  
980 39.

981 Boulton, A.J., Findlay, S., Marmonier, P., Stanley, E.H., Valett, H.M. (1998). The functional  
982 significance of the hyporheic zone in streams and rivers. *Annual Review of Ecology &*  
983 *Systematics* 29: 59–81, doi: 10.1146/annurev.ecolsys.29.1.59

984 Bourke, S.A., Cook, P.G., Shanafield, M., Dogramaci, S., Clark, J.F. (2014). Characterisation of  
985 hyporheic exchange in a losing stream using radon-222. *Journal of Hydrology* 519: 94–105,  
986 doi:10.1016/j.jhydrol.2014.06.057.

987 Bristow, C.S., Best, J.L. (1993) Braided rivers: perspectives and problems. From: Best, J.L. and  
988 Bristow, C.S. (eds) *Braided Rivers*, Geological Society, London, Special Publications. Volume  
989 75 Pages 1-11, doi:10.1144/GSL.SP.1993.075.01

990 Brower, A., Hoyle, J., Gray, D., Buelow, F., Calkin, A., Fuller, I., Gabrielson, R., Grove, P.,  
991 Brierley, G., Sai-Louie, A.J., Rogers, J., Shulmeister, J., Uetz, K., Worthington, S., Vosloo, R.  
992 (2024). New Zealand's braided rivers: The land the law forgot. *Earth Surface Processes and*  
993 *Landforms* 49 (1): 10–14, doi: 10.1002/esp.5728

994 Brunner, P., Cook, P.G., Simmons, C.T., (2009a), Hydrogeologic controls on disconnection  
995 between surface water and groundwater, *Water Resource. Res.*, 45(1), 1–13, W01422,  
996 doi:10.1029/2008WR006953

997 Brunner, P., Simmons, C.T., Cook, P.G. (2009b). Spatial and temporal aspects of the  
998 transition from connection to disconnection between rivers, lakes and groundwater. *Journal*  
999 *of Hydrology* 376 (1–2): 159–169, doi:10.1016/j.jhydrol.2009.07.023.

1000 Brunner, P., Simmons, C.T. (2012). Hydrogeosphere: A Fully Integrated, Physically Based  
1001 Hydrological Model. *Groundwater* 50: 170-176, doi:10.1111/j.1745-6584.2011.00882

1002 Brunner, P., Therrien, R., Renard, P., Simmons, C.T., Hendricks Franssen, H.-J. (2017).  
1003 Advances in understanding river-groundwater interactions. *Reviews of Geophysics* 55: 818-  
1004 854 doi:10.1002/2017RG000556

1005 Cardenas, M.B., Zlotnik, V.A. 2003. Three-dimensional model of modern channel bend  
1006 deposits. *Water Resources Research* 39: 1141, doi:10.1029/2002WR001383

1007 Cartwright, I., Hoffmann, H. 2016. Using radon to understand parafluvial flows and the  
1008 changing locations of groundwater inflows in the Avon River, southeast Australia. *Hydrology*  
1009 *& Earth Systems Sciences* 20: 3581–3600, doi:10.5194/hess-20-3581-2016

1010 Coluccio, K., Morgan, L. K. (2019). A review of methods for measuring groundwater-surface  
1011 water exchange in braided rivers. *Hydrology & Earth Systems Sciences* 23: 4397–4417,  
1012 doi:10.5194/hess-23-4397-2019

1013 Di Ciacca, A., Leterme, B., Laloy, E., Diederik, D., Vanderborght, J. (2019). Scale-dependent  
1014 parameterization of groundwater–surface water interactions in a regional hydrogeological  
1015 model. *Journal of Hydrology* 576: 494-507, doi:10.1016/j.jhydrol.2019.06.072.

1016 Di Ciacca, A., Wilson, S., Kang, J., Wöhling, T. (2023). Deriving transmission losses in  
1017 ephemeral rivers using satellite imagery and machine learning. *Hydrology & Earth Systems*  
1018 *Sciences* 27: 703-722, doi:10.5194/hess-27-703-2023

1019 Dravid P.N., Brown L.J., 1997. Heretaunga Plain Groundwater Study - Vol 1: Findings.  
1020 Hawke's Bay Regional Council, 254p.

1021 Durejka, S., Gilfedder, B., Frei, S. (2019). A method for long-term high resolution <sup>222</sup>Radon  
1022 measurements using a new hydrophobic capillary membrane system. *Journal of*  
1023 *Environmental Radioactivity* 208-209: 105980, doi:10.1016/j.jenvrad.2019.05.012.

1024 Durrige (2020a). RAD7 electronic radon detector user manual.

1025 Durrige (2020b). RAD H2O Radon in Water accessory for the RAD7 User Manual.

1026 Durrige (2020c). Continuous Radon in Water Accessory for the RAD7 user manual.

1027 Durrige. (2021). DRYSTIK Models ADS-3 and ADS-3R Active Moisture Exchanger Accessory  
1028 for the RAD7 User Manual

1029 Folk R.L., Ward W.C., 1957. Brazos River bar: a study in the significance of grain size  
1030 parameters. *Journal of Sedimentary Petrology* 27: 3–26.

1031 Forsyth, P.J., Barrell, D.J.A., Jongens, R. (compilers) (2008). Geology of the Christchurch area.  
1032 Institute of Geological & Nuclear Sciences 1:250 000 geological map 16. 1 sheet + 67p.  
1033 Lower Hutt, New Zealand. GNS Science.

1034 Fox, G.A., Durnford, D.S., 2003. Unsaturated hyporheic zone flow in stream conjunctive  
1035 systems. *Advances in Water Resources* 26 (9), 989–1000.

1036 Gardner, M., Sharma, N., 2016. Wairau River Mean Bed Level and Volumetric Analysis: 2010  
1037 to 2016. Report to Marlborough District Council, 57p.

1038 González-Pinzón, R., Ward, A.S., Hatch, C.E., Wlostowski, A.N., Singha, K., Gooseff, M.N.,  
1039 Haggerty, R., Harvey, J.W., Cirpka, O.A., Brock, J.T. (2015). A field comparison of multiple  
1040 techniques to quantify groundwater-surface-water interactions. *Freshwater Science* 34: 139-  
1041 160, doi:10.1086/679738

1042 Gray DP, Hicks M, Greenwood M 2016. Advances in geomorphology and aquatic ecology of  
1043 braided rivers. In Jellyman PG, Davie TJA, Pearson CP, Harding JS. (Eds) Advances in New  
1044 Zealand freshwater science. New Zealand Freshwater Sciences Society, Christchurch, New  
1045 Zealand. Pp 357-378.

1046 Harbaugh, A.W. (2005). MODFLOW-2005, the U.S. Geological Survey modular ground-water  
1047 model -- the Ground-Water Flow Process: U.S. Geological Survey Techniques & Methods 6-  
1048 A16.

1049 Harvey, J., Gooseff, M. (2015). River corridor science: Hydrologic exchange and ecological  
1050 consequences from bedforms to basins. *Water Resources Research* 51: 6893–6922,  
1051 doi:10.1002/2015WR017617.

1052 Harvey, J.W., Wagner, B.J. (2000). Quantifying Hydrologic Interactions between Streams and  
1053 Their Subsurface Hyporheic Zones. In: Jones, J.B. and Mulholland, P.J. (eds) Streams and  
1054 ground waters. San Diego, CA: Academic Press, pp. 3–44, doi: 10.1016/B978-012389845-  
1055 6/50002-8.

1056 Holmes, R. M., Fisher, S. G., & Grimm, N. B. (1994). Parafluvial Nitrogen Dynamics in a  
1057 Desert Stream Ecosystem. *Journal of the North American Benthological Society*, 13 (4): 468–  
1058 478, doi:10.2307/1467844

1059 Huber, E., Huggenberger, P. (2016). Subsurface flow mixing in coarse, braided river deposits.  
1060 *Hydrology & Earth Systems Sciences* 20: 2035–2046, doi:10.5194/hess-20-2035-2016

1061 Huggenberger, P., Hoehn, E., Beschta, R., Woessner, W. (1998). Abiotic aspects of channels  
1062 and floodplains in riparian ecology. *Freshwater Biology* 40: 407-425, doi:10.1046/j.1365-  
1063 2427.1998.00371.x

1064 Huggenberger P., Regli, C. (2006). A sedimentological model to characterise Braided River  
1065 deposits for hydrogeological applications. In: Sambrook Smith GH (ed) Braided rivers:  
1066 process, deposits, ecology and management. Blackwell, Malden, MA, pp 51–74.

1067 Hupp, C.R., Osterkamp, W.R. 1996. Riparian vegetation and fluvial geomorphic processes.  
1068 *Geomorphology* 14: 277-295.

1069 Kalbus, E., Reinstorf, F., Schirmer, M., 2006. Measuring methods for groundwater-surface  
1070 water interactions: a review. *Hydrology & Earth System Sciences* 10: 873-887  
1071 doi:10.5194/hess-10-873-2006

1072 Khambhammettu, P., Renard, P., & Doherty, J. (2020). The traveling pilot point method. A  
1073 novel approach to parameterize the inverse problem for categorical fields. *Advances in*  
1074 *Water Resources* 138: 103556, doi:10.1016/j.advwatres.2020.103556.

1075 Larned, S. T., Hicks, D. M., Schmidt, J., Davey, A. J. H., Dey, K., Scarsbrook, M., Arscott, D. B.,  
1076 Woods, R. A. (2008). The Selwyn River of New Zealand: A benchmark system for alluvial  
1077 plain rivers. *River Research & Applications* 24, 1–21, doi:10.1002/rra.1054

1078 Laube, G., Schmidt, C., Fleckenstein, J.H. (2018). The systematic effect of streambed  
1079 conductivity heterogeneity on hyporheic flux and residence time. *Advances in Water*  
1080 *Resources* 122: 60-69, doi:10.1016/j.advwatres.2018.10.003

1081 Lee, J.M, Bland, K.J., Townsend, D.B., Kamp, P.J. J. (compilers) (2011). Geology of the  
1082 Hawkes Bay area. Institute of Geological & Nuclear Sciences 1:250 000 geological map 8. 1  
1083 sheet + 93p. Lower Hutt, New Zealand. GNS Science.

1084 Levy, J., Birck, M. D., Mutiti, S., Kilroy, K. C., Windeler, B., Idris, O., & Allen, L. N. (2011). The  
1085 impact of storm events on a riverbed system and its hydraulic conductivity at a site of  
1086 induced infiltration. *Journal of Environmental Management*, 92: 1960–1971,  
1087 doi:10.1016/j.jenvman.2011.03.017

1088 Measures, R. (2012). Modelling gravel transport, extraction and bed level change in the  
1089 Ngaruroro River. NIWA Client Report CHC2012-121 for Hawkes Bay Regional Council.

1090 Montgomery, J., Bind, J., Measures, R., Hoyle, J. (subm.). Novel methods for measuring  
1091 porosity in gravel bed rivers. *Water Resources Research*.

1092 Morel-Seytoux, H.J., Miller, C.D., Mehl, S. and Miracapillo, C. (2018) Achilles' heel of  
1093 integrated hydrologic models: The stream-aquifer flow exchange, and proposed alternative.  
1094 *Journal of Hydrology* 564, 900-908.

1095 Niswonger, R.G., Prudic, D.E. (2005). Documentation of the Streamflow-Routing (SFR2)  
1096 Package to include unsaturated flow beneath streams - A modification to SFR1: U.S.  
1097 Geological Survey Techniques and Methods 6-A13, 50 p.

1098 Pirot, G., Huber, E., Irving, J., Linde, N. (2019). Reduction of conceptual model uncertainty  
1099 using ground-penetrating radar profiles: Field-demonstration for a braided-river aquifer.  
1100 *Journal of Hydrology* 571: 254-264, doi:10.1016/j.jhydrol.2019.01.047

1101 Pirot, G., Straubhaar, J., and Renard, P. (2014). Simulation of braided river elevation model  
1102 time series with multiple-point statistics. *Geomorphology* 214: 148–156,  
1103 doi:10.1016/j.geomorph.2014.01.022

1104 Pirot, G., Straubhaar, J., Renard, P. (2015). A pseudo genetic model of coarse braided-river  
1105 deposits. *Water Resources Research* 51: 9595-9611, doi:10.1002/2015WR017078.

1106 Poole, G.C., Berman, C.H. (2001). An ecological perspective on in-stream temperature:  
1107 natural heat dynamics and mechanisms of human-caused thermal degradation.  
1108 *Environmental Management* 27: 787-802, doi:10.1007/s002670010188

1109 Pryshlak, T.T., Sawyer, A.H., Stonedahl, S.H., Soltanian, M.R. (2015). Multiscale hyporheic  
1110 exchange through strongly heterogeneous sediments. *Water Resources Research* 51: 9127–  
1111 9140, doi:10.1002/2015WR017293.

1112 Rawlinson, Z.J, Westerhoff, R.S., Foged, N., Kellett, R.L. (2021). Hawke’s Bay 3D Aquifer  
1113 Mapping Project: Heretaunga Plains SkyTEM data processing and resistivity models. GNS  
1114 Science Consultancy Report 2021/93

1115 Reinfelds, I., Nanson, G. (1993), Formation of braided river floodplains, Waimakariri River,  
1116 New Zealand. *Sedimentology* 40: 1113-1127. [https://doi.org/10.1111/j.1365-](https://doi.org/10.1111/j.1365-3091.1993.tb01382.x)  
1117 [3091.1993.tb01382.x](https://doi.org/10.1111/j.1365-3091.1993.tb01382.x)

1118 Rushton, K. (2007) Representation in regional models of saturated river–aquifer interaction  
1119 for gaining/losing rivers. *Journal of Hydrology* 334(1), 262-281.

1120 Schälchli, U. (1992). The clogging of coarse gravel river beds by fine sediment. *Hydrobiologia*  
1121 235/236(1):189–197

1122 Schilling, O. S., Partington, D. J., Doherty, J., Kipfer, R., Hunkeler, D., & Brunner, P. (2022).  
1123 Buried paleo-channel detection with a groundwater model, tracer-based observations, and  
1124 spatially varying, preferred anisotropy pilot point calibration. *Geophysical Research Letters*,  
1125 49 (14): e2022GL098944. <https://doi.org/10.1029/2022GL098944>

1126 Shanafield, M., Cook, P.G. (2014). Transmission losses, infiltration and groundwater  
1127 recharge through ephemeral and intermittent streambeds: A review of applied methods.  
1128 *Journal of Hydrology* 511: 518–529, doi:10.1016/j.jhydrol.2014.01.068

1129 Shanafield, M., Bourke, S.A., Zimmer, M.A., Costigan, K.H. (2021). An overview of the  
1130 hydrology of non-perennial rivers and streams. *WIREs Water* 8: e1504,  
1131 doi:10.1002/wat2.1504Fsongol

1132 Songola, C. (2022). Characterising Surface Water and Groundwater Interactions in Braided  
1133 Rivers Using Hydraulics and Environmental Tracers: The Waikirikiri Selwyn River. MSc thesis,  
1134 Lincoln University.

1135 Sophocleous, M. (2002). Interactions between groundwater and surface water: The state of  
1136 the science. *Hydrogeology Journal* 10 (1): 52-67, doi:10.1007/s10040-001-0170-8

1137 Stanford, J.A. & Ward, J. V. (1993). An Ecosystem Perspective of Alluvial Rivers: Connectivity  
1138 and the Hyporheic Corridor. *Journal of the North American Benthological Society* 12 (1): 48-  
1139 60.

1140 Steiger, J., Tabacchi, E., Dufour, S., Corenblit, D., Peiry, J.-L. (2005), Hydrogeomorphic  
1141 processes affecting riparian habitat within alluvial channel–floodplain river systems: a



1142 review for the temperate zone. *River Research and Applications* 21: 719-737,  
1143 doi:10.1002/rra.879

1144 Tang, Q., Schilling, O. S., Kurtz, W., Brunner, P., Vereecken, H., & Hendricks Franssen, H.-J.  
1145 (2018). Simulating flood induced riverbed transience using unmanned aerial vehicles,  
1146 physically-based hydrological modelling and the ensemble Kalman filter. *Water Resources*  
1147 *Research* 54: 9342–9363, doi:10.1029/2018WR023067.

1148 Theel, M., Huggenberger, P., Zosseder, K. (2020). Assessment of the heterogeneity of  
1149 hydraulic properties in gravelly outwash plains: a regionally scaled sedimentological analysis  
1150 in the Munich gravel plain, Germany. *Hydrogeology Journal* 28: 2657–2674,  
1151 doi:10.1007/s10040-020-02205-y

1152 Therrien, R., McLaren, R. G., Sudicky, E. A., Panday, S. M. (2010). *HydroGeoSphere: A Three-*  
1153 *dimensional Numerical Model Describing Fully-integrated Subsurface and Surface Flow and*  
1154 *Solute Transport*. Groundwater Simulations Group, University of Waterloo. 443 p.

1155 Valett, H.M, Morrice, J.A., Dahm, C.N., Campana, M.E. (1996). Parent lithology, surface–  
1156 groundwater exchange, and nitrate retention in headwater streams. *Limnology and*  
1157 *Oceanography* 41: doi: 10.4319/lo.1996.41.2.0333.

1158 Warburton, J. (1996). Active braidplain width, bed load transport and channel morphology  
1159 in a model braided river. *Journal of Hydrology (New Zealand)*, 35(2), 259–285.  
1160 <http://www.jstor.org/stable/43944775>

1161 Ward, A.S. (2015). The evolution and state of interdisciplinary hyporheic research. *WIREs*  
1162 *Water* 3: 83-103, doi:10.1002/wat2.1120

1163 Ward, A.S., Packman, A.I. (2019). Advancing our predictive understanding of river corridor  
1164 exchange. *WIREs Water* 6: doi:10.1002/wat2.1327

1165 White, D.S. (1993). Perspectives on defining and delineating hyporheic zones. *Journal of the*  
1166 *North American Benthological Society* 12: pp. 61– 69.

1167 White, P.A., Kovacova, E., Zemansky, G., Jebbour, N., Moreau-Fournier, M. (2012).  
1168 Groundwater-surface water interaction in the Waimakariri River, New Zealand, and  
1169 groundwater outflow from the river bed. *Journal of Hydrology (NZ)* 51: 1-23.

1170 Wöhling, T., Gosses, M.J., Wilson, S.R., Davidson, P. (2018). Quantifying river–groundwater  
1171 interactions of New Zealand’s gravel-bed rivers: The Wairau Plain. *Groundwater*, 56: 647–  
1172 666, doi:10.1111/gwat.12625

1173 Wöhling, T., Wilson, S.R., Wadsworth, V., Davidson, P. (2020). Detecting the cause of change  
1174 using uncertain data: Natural and anthropogenic factors contributing to declining  
1175 groundwater levels and flows of the Wairau Plain aquifer, New Zealand. *Journal of*  
1176 *Hydrology: Regional Studies* 31:100715, doi:10.1016/j.ejrh.2020.100715

1177 Wu, G.D., Shu, L.C., Lu, C.P., Chen, X.H., Zhang, X. Appiah-Adjei, E.K., Zhu, J.S. (2015).  
1178 Variations of streambed vertical hydraulic conductivity before and after a flood season.  
1179 *Hydrogeology Journal* 23: 1603-1615 doi:10.1007/s10040-015-1275-9

1180 Wu, F.-C & Huang, H.-T. (2000). Hydraulic Resistance Induced by Deposition of Sediment in  
1181 Porous Medium. *Journal of Hydraulic Engineering* 126 (7): 547-551

1182 Zhou, Y., Ritzi, R.W., Soltanian, M.R., Dominic, D.F. (2014). The influence of streambed  
1183 heterogeneity on Hyporheic flow in gravelly Rivers. *Groundwater* 52: 206–216,  
1184 doi:10.1111/gwat.12048